Princetonlaan 6
3584 CB Utrecht
Postbus 80015
3508 TA Utrecht

www.tno.nl

T +31 88 866 42 56
F +31 88 866 44 75

TNO-rapport

Transport of atmospherically deposited PFAS in selected Dutch soils.

Datum	12 februari 2021
Auteur(s)	T.G.J.Gerardu
Exemplaarnummer	1
Oplage	0
Aantal pagina's	74 (incl. bijlagen)
Aantal bijlagen	5
Opdrachtgever	TNO
Projectnaam	PFAS onderzoek
Projectnummer	060.43320/01.01.06.

Princetonlaan 6
3584 CB Utrecht
Postbus 80015
3508 TA Utrecht

www.tno.nl

T +31 88 866 42 56
F +31 88 866 44 75

Sorptive transport of atmospherically deposited PFAS in selected Dutch soils.
Thomas Gerardu – 5533708
Date: 12-01-2021
Supervisors: Prof. dr. Jasper Griffioen (TNO & UU) and Dr. ir. Joris Dijkstra (TNO).
Second reader: Dr. Iris Pitt (UU).

Samenvatting

Poly- en perfluoralkylstoffen (PFAS) zijn oppervlakte-actieve stoffen die gebruikt zijn (en worden) in een groot aantal consumentenproducten en productieprocessen. De groep bestaat uit zo'n 6000 stoffen, waarvan perfluoroctaanzuur (PFOA) en perfluorooctaansulfonaat (PFOS) de bekendste zijn. Het wordt steeds duidelijker dat ze bio-accumulerend, giftig en moeilijk te verwijderen zijn. De aanleiding voor dit onderzoek is de PFAS problematiek die het grondverzet in 2019 grotendeels heeft stilgelegd en tot grote maatschappelijke onrust heeft geleid. De Chemours fabriek in Dordrecht heeft als enige in Nederland PFOA gebruikt van 1970-2012 bij het produceren van Teflon en Viton. Ook is bekend dat PFOA is uitgestoten via de lucht en dat het terecht is gekomen in de nabijheid van de fabriek (vooral in een 50 km radius).

De eerste onderzoeksvraag was wat het effect is van bodemeigenschappen op het transport van PFOA en PFOS in de bodem. Daarbij is onderzocht of er een gehalte-diepte profiel zichtbaar is en of er een verschil is tussen deze profielen in verschillende type bodems. De tweede onderzoeksvraag was of de gehalte-diepte profielen consistent zijn met de emissie van Chemours in de jaren 1970-2012 en of een hydrologische model (HYDRUS-1D) gebruikt kan worden om PFAS transport in de bodem te modelleren.

Om dit te onderzoeken is er veldwerk verricht waarbij 40 grondmonsters zijn genomen op vier verschillende locaties in de Alblasserwaard. De locaties zijn gekozen op vier aspecten, namelijk benedenwinds van Chemours, in ongeroerde grond, met verticale infiltratie van regenwater en een (zoveel mogelijk) homogene bodem. De monsters zijn geanalyseerd op organisch materiaal- (OM) en organisch koolstofgehalte (OC), korrelgrootteverdeling, PFOA- en PFOS-gehalte. De resultaten van deze analyses zijn gebruik voor het op onafhankelijke wijze specificeren van parameters van HYDRUS.

De gemeten resultaten laten zien dat in zandige bodems, PFOA en PFOS ophopen in de bovenste bodemlaag, specifiek daar waar het OM gehalte het hoogst is. PFOA komt in hogere gehaltes voor dan PFOS. PFOA komt voor tot 4.2 µg/kg dry soil (ds) in zand en 27 µg/kg ds in veen. PFOS komt voor tot 1.1 µg/kg ds in zand en 6.8 µg/kg ds in veen. In de veenbodem zijn OM en OC een stuk hoger dan in de zandbodems. PFOA en PFOS reiken minder diep in veenbodems dan in de zandbodems. De modelresultaten, verkregen met onafhankelijk bepaalde inputgegevens en literatuur-ranges van interactieparameters tussen PFAS en OC, laten een bandbreedte aan gesimuleerde gehalte-diepte profielen zien. De gemeten gehalte-diepte profielen liggen vaak in het berekende bereik. De gehalte-diepte profielen van PFOS laten niet direct een verband zien met de historische uitstoot van Chemours. Een vervolgonderzoek, met een zelfde opzet als dit onderzoek, zou zich kunnen richten op het mogelijke verband tussen de afvalverbrandingsinstallatie (ATM) in Moerdijk en PFOS in de bodem in dit gebied.

De conclusies zijn ten eerste dat er een duidelijk PFAS gehalte-diepte profiel aanwezig is. Een identieke depositie geschiedenis met verschillende bodemtypes op dezelfde geografische locatie levert verschillende gehalte-diepte profielen op. De ophoping van PFAS hangt sterk samen met het OM/OC gehalte in de bodem. De modelsimulaties zijn tot stand gekomen met onafhankelijk bepaalde inputgegevens en laten zeer grote overeenkomsten zien met de gemeten resultaten. Hierdoor is het zeer aannemelijk dat PFOA in de grondmonsters afkomstig is van Chemours waarbij de emissie historie een goede verklaring biedt voor de resultaten.

Summary

Poly- and perfluoro-alkyl substances (PFAS) are surfactants that were (and are) used in a large number of consumer products and production processes. The group consists of about 6,000 substances of which perfluorooctanoic acid (PFOA) and perfluorooctane sulfonate (PFOS) are the best known. PFAS are bioaccumulative, toxic and difficult to remove from soil once they end up in the environment. The incentive for this study is the problem of PFAS, which largely halted construction projects 2019 and led to the concern about PFAS in our society. The Chemours factory in Dordrecht in the Netherlands was the only one to utilize PFOA from 1970-2012 in the production of Teflon and Viton. PFOA was emitted into the air and was deposited in the vicinity of the plant (especially within a 50 km radius).

The first research question was what the effect is of soil properties on the transport of PFOA and PFOS in the soil. It was investigated whether a content-depth profile is observed and whether there is a difference between these profiles in different types of soils. The second research question was whether the content-depth profiles are consistent with the emission of Chemours in the years 1970-2012 and whether a hydrological model (HYDRUS-1D) could be used to model PFAS transport in soil. To investigate this, fieldwork was carried out to collect 40 soil samples at four different locations in the Alblasserwaard. The locations were chosen on four aspects, namely downwind of Chemours, in undisturbed soil, vertical infiltration of rainwater and (as much as possible) homogeneous soil. The samples were analysed on organic material- (OM) and organic carbon content (OC), grain size distribution, PFOA and PFOS content. The results of these analyses have been used to independently specify input parameters for HYDRUS.

The measured results show that in sandy soils, PFOA and PFOS accumulate in the top soil layer, specifically where the OM content is highest. The PFOA contents is in all soil samples higher than the PFOS content. PFOA contents are up to 4.2 µg/kg dry soil (ds) in sand and 27 µg/kg ds in peat. PFOS contents are up to 1.1 µg/kg ds in sand and 6.8 µg/kg ds in peat. OM and OC are much higher in the peat soil than in the sandy soils. PFOA and PFOS reach less deep in peat soils than in sandy soils. The model input data was independently determined and interaction parameter for PFAS & OC were collected from literature. The model results show a range of simulated content-depth profiles. The measured content-depth profiles are often within the calculated range of simulated content-depth profiles. The content-depth profiles of PFOS do not show a direct relationship with the historical emissions of Chemours. A follow-up study, with the same set-up as this study, could investigate the relation between the waste incineration plant (ATM) in Moerdijk and PFOS in the soil in this area.

The conclusions are firstly that there is a clear PFAS content-depth profile. An identical deposition history with different soil types at the same geographic location yields different content-depth profiles. The accumulation of PFAS is strongly related to the OM/OC content in the soil. The model simulations have been created with independently determined input data and show very close correspondences with the measured results. This makes it very likely that the PFOA in the soil samples originates from Chemours, where the emission history provides a good explanation for the results.

Table of contents

List of Figures:

List of Tables:

1 Introduction

1.1 Background

Pollution of soil by anthropogenic compounds can form a threat to human, animal, plant and microorganism life. Soil pollution occurs if the concentration of a certain substance (the pollutant or contaminant) exceeds the natural background value that normally occurs in that environment. Since pollution of the environment including the soil is unwanted, the production, application and disposal of a large group of pollutants is regulated by law.

Since the 1960s, a lot of new substances have been invented that are used in a large variety of products (Lindstrom et al., 2011). One of those substances is PFAS, which is an acronym for Per- and polyFluoroAlkyl Substances. This group of substances is characterized by its unique surface-active properties. PFAS are both water and oil repellent and they are highly resistant to heat and acids (Pancras et al., 2018). The industry has developed many different variations which resulted in a group of more than 6,000 different compounds (Pancras et al., 2018). The application of these compounds in industrial or household products is very wide. They are used as stain protection in carpets, water-repellent coating for textiles, metal-working processes, to produce non-stick materials and certain types of fire-fighting foams (Pancras et al., 2018).

Since 2000, the substances from the PFAS group have come under increasing attention because scientific research shows that these substances are persistent, bioaccumulative and toxic (Buck et al., 2011). In addition, environmental monitoring shows that these substances are frequently present in our environment (Zareitalabad al., 2013). The majority of these substances is not routinely measured (Pancras et al., 2018). The past few years, awareness has grown of the possibly negative health effects of (long-term) exposure to PFAS. PFAS has come under increasing attention in the media, often called a ‘forever chemical’ (Gibbens, 2021). A few northern European countries, among which the Netherlands, submitted a proposal to the European Chemical Agency (ECHA) to restrict the production and use in the European Union and to add the chemical to the Registration, Evaluation, Authorisation and Restriction of Chemicals (REACH) database (ECHA, 2021).

1.2 Focus and scope

In the Netherlands, only one factory has used a type of PFAS for the production of a number of products, which is the Chemours factory (formerly DuPont) in Dordrecht, province of South-Holland. They mainly used PFOA and likely PFOS, which are the two most common types of PFAS, for the production of Teflon and Viton between 1970 and 2012 (Pancras et al., 2018; Koch et al., 2017). The atmospheric emissions of the factory spread across the Netherlands during this period and were deposited on soil and in surface waters by means of dry and wet deposition (van Bentum et al., 2017). PFOA was also released from the factory in surface waters as effluent (Pancras et al., 2018). The most severe regional pollution is found within a 50 km radius of the factory in Dordrecht (Wintersen et al., 2020).

However, there are many local sources of PFAS pollution in densely populated areas in the Netherlands (e.g. through landfills, waste incineration facilities and fire brigade training areas). This research focusses specifically on the effects of the historical deposition on the accumulation of PFAS in undisturbed, agricultural Dutch soils within the vicinity of the factory (within 50 km radius). More specifically, it will focus on two types of PFAS: PFOS and PFOA.

1.3 Relevance and problem definition

Environment and health
PFAS is a non-degrading group of pollutants that has spread to every place on earth (Calafat et al., 2006). Ninety-eight percent of Americans have traceable levels of PFAS in their blood (Calafat et al., 2006).. Exposure of PFAS to people mainly occurs through drinking water or food (Noorlander et al., 2010; Pérez et al., 2014). Known health issues if exposed to unsafe levels of PFAS include birth weight problems, perturbation in the immune system, multiple types of cancers and hormone disruptions (Sunderland et al., 2019). PFAS are bioaccumulative but they can be broken down in the body (Pancras et al., 2018). They bind to proteins (as opposed to other common pollutants which bind to fat-tissue) and their excretion can be slow. The half-life time for PFOS and PFOA in the human body can be 3-4 years and 2-3 years, respectively (Olsen et al., 2007). PFOA has been found in increased concentrations in the blood of residents living near the factory in Dordrecht (Poll et al., 2017). The people living in the very close vicinity (< 1 km) of the factory were exposed to atmospheric PFOA concentrations above the safety standard set by the RIVM for over 25 years (Zeilmaker et al., 2016).

Infrastructure
In June 2019, the Dutch government decided to set a generic background value of 0.1 µg/kg for PFAS, being a novel emerging contaminant, in soil (Pancras et al., 2018). This was done to limit the spreading of PFAS-polluted soil to unpolluted areas. The so-called background value of 0.1 µg/kg corresponded to the detection limit, as the true background value of PFAS in Dutch soil was not sufficiently known and assumed to be negligible. However, it appeared that high percentages of excavated soil and dredged sediments, even those that were “unsuspected” with respect to PFAS pollution, contained PFAS contents higher than the background value. This resulted in disruption in the dredging and construction sectors, as previously unsuspected soil was now classified as polluted and could not be moved anymore. Many of the construction projects were delayed, which had financial implications for the companies working in those sectors. Subsequently, the National Institute for Public Health and Environment (RIVM) investigated the national spreading of PFAS in the Dutch top- and subsoil (Pancras et al., 2019). It was found that most of the top soils in the Netherlands (89%) contains PFAS above the background value of 0.1 µg/kg soil. By the end of 2019, the background value was set to 0.8 µg/kg for PFOA and 0.9 µg/kg for PFOS (Wintersen et al., 2019). In July 2020, the background values were raised to 1.4 and 1.9 µg/kg for PFOS and PFOA, respectively, based on additional, systematic monitoring research at national scale (RIVM, 2021). The new value is expected to solve the most urgent problems for the construction sector.

Previous Dutch research on PFAS in the environment
In 2011, the Expertisecentrum PFAS was founded by the consultancy companies Arcadis, TTE Consultants and Witteveen+Bos because there was an urge to know more about PFAS and the spread of it in the Netherlands. PFAS is a relatively new problem in the Netherlands. Structured and accessible information on these substances was scarce or lacking. In 2016 and onwards, the Expertisecentrum carried out a number of studies. Zeilmaker et al. (2016) did a risk assessment on PFOA exposure to residents of Dordrecht. Van Bentum et al. (2017) did research on the deposition of PFOA and Gen-X in Dordrecht and surrounding. Poll et al. (2017) carried out PFOA measurements in blood of people living close to the Chemours factory. The transport of PFOA by emission into air and deposition in the surrounding landscape was 'highly likely' (van Bentum et al., 2017). Although the factory has turned to the use of Gen-X instead of PFOA in 2012, recent analysis of soil samples (after 2018) still found elevated PFOA content in the top- and subsoil down to a depth of 0.5 m, even at locations where it was not expected (Brandsma et al., 2019).

Knowledge gap
In short, the scientific literature on the spreading and the fate of PFAS in the Netherlands is rather limited (Zeilmaker et al., 2016; van Bentum et al., 2017; Pancras et al., 2018; Expertisecentrum PFAS, 2018; Wintersen et al., 2019). The investigations have focused on spatial occurrence of PFAS in the Dutch environment and on the exposure and health risks of inhabitants of Dordrecht that live in the vicinity of the Chemours factory. The emphasis in the pre-mentioned studies was more towards quantifying the spread. This is reflected in the sample interval in those studies, where 1-3 samples per location were taken (van Bentum et al.,2017; Expertisecentrum PFAS, 2018).

Relatively unexplored is how PFAS in the soil behaves over time, if there is a content-depth profile visible in the soil, whether it leaches into groundwater and if so, at what rate. More specifically it is unknown how PFAS originating from the Chemours factory infiltrates in the Dutch soil, as governed by the historical PFAS atmospheric deposition, rainfall, and hydrological and chemical soil properties.

1.4 Objectives and research questions

This research aims to characterise the extent of PFAS contamination at selected undisturbed sites as a result of atmospherically deposited PFAS from the Chemours factory. More specifically it aims to understand the influence of soil properties on the transport PFOS and PFOA in rural Dutch soils in areas downwind of Chemours in Dordrecht where the deposition has been shown to be the highest (Zeilmaker et al., 2016; van Bentum et al., 2017). Secondly, it aims to investigate whether the content-depth profiles from borehole cores taken from undisturbed sites can be explained by the emission history from the Chemours factory.
The first hypothesis is that the emission history of the factory can be related to the PFAS content in a vertical soil profile in the vicinity. From what is known from literature, it is hypothesized that the vertical variation of PFAS content in soil shows trends in the deposition history of PFAS (Qi et al., 2015).

In other words, the depth profile of PFAS content can be used as an historical archive of atmospheric emission.
If this is true, we may expect to see a certain PFAS content at ground level, followed by an increase in content (historic deposition of PFAS) followed by a decrease in content (time before PFAS was emitted). The second hypothesis is that in two adjacent but different soil types (sand versus peat soil), the amount of infiltrated PFAS is similar but the infiltration depth is considerably smaller at the peat soil. On top of that it is hypothesized that increasing distance from the source results in lower cumulative PFAS content in the soil.

The scientific relevance of this research lies in new knowledge about PFAS accumulation in Dutch soil in general and as a result of atmospheric deposition in relation to Chemours. It will generate more insight as to how long historically deposited PFAS remains in the soil and what this pollution looks like in terms of quantity and depth. This useful information for long-term risk assessments.
If it is possible to establish a relation between the PFAS content in the soil and the emission history, this relation can be used to roughly predict what the PFAS content would be in other places with atmospheric deposition as transport route. This could be helpful to explain deviations between ‘expected’ pollution from historical deposition and other, more locally generated pollution (for example a waste plant and/or fire extinguish event). A hydrological model will be used for this.

The societal relevance of this topic is substantial as PFAS pollution is a current theme that concerns people’s health. There is a concern if/and how much people are exposed to PFAS and the frequent news articles in newspapers and other media are an example of this (YubaNet, 2021; Favors, 2021). For the people living near the Alblasserwaard, this research gives insight into the degree of soil pollution they live with. Knowledge about the behaviour of PFAS in the soil in this region can be used by people who want to use or cultivate the land. Lastly this research explores the potential to use hydrological models to better understand PFAS transport in soils. Potentially, the model could be used to calculate how much PFAS pollution can be expected in this region. This has economic benefits as use of models is often much cheaper than field research.

Two research questions are posed to capture the objectives of this research:

1. What is the effect of soil properties on the occurrence of PFAS in the unsaturated zone?
    a. Is there a clear content-depth profile of PFAS measurable in the selected soils?
    b. Is there a notable difference in the content-depth profile of PFAS in different soil types that have undergone a presumably similar atmospheric deposition of PFAS?

2. Can the deposition profile of PFAS be linked to the historical emission of PFAS by the Chemours factory in Dordrecht?
    a. Can HYDRUS-1D be used to simulate emission history of the Chemours factory?

It should be noted that this research has an exploratory character. In the context of this research that means that the above hypotheses on the relation between historical emissions and content-depth profiles of PFAS in soil will not be tested in a statistical manner, but its likeliness is further determined by means of a combination of literature study, fieldwork, sample analysis and water- and solute transport modelling.

1.5 Reading guide

Chapter 2 describes PFAS more in depth in terms of chemical properties, uses and their occurrence in the environment. Chapter 3 describes the field and laboratory methods that were used and how a hydrological model was used to simulate PFAS transport in soil. The results are presented in Chapter 4. Chapter 5 is used to discuss the results on significance, interpretation and in context with other research. Conclusions are drawn in Chapter 6.

This research focusses on PFOS and PFOA. If PFAS is mentioned in Chapter 3-6, both PFOS and PFOA are meant.

2 Background

There are many PFAS. This chapter will focus mostly on the PFOS and PFOA as these are relevant for this research.

2.1 Types and environmental properties of PFAS

2.1.1 Types

PFAS is a group of man-made Poly- and Perfluorinated Alkyl Substances with a large variety of up to 6,000 individual substances (Pancras et al., 2018). All PFAS contain a complete (per-) or partially (poly-) fluorinated carbon chain with varying length of 2 to 16 carbon atoms. In per-fluorinated molecules, all H atoms are replaced by F atoms. In polyfluorinated molecules, not all H atoms are replaced by F atoms, see Figure 1.

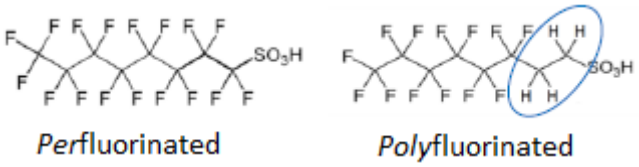

Figure 1. Per- and Polyfluorinated molecule example.

Buck et al. (2011) defined PFAS as substances that contain the unit C_nF_{2n+1}. To keep an overview of this large group, it has been divided in 42 families. Figure 2 shows a strongly simplified diagram of non-polymer PFAS. Simply put, PFAS consist a fluorinated carbon chain and a functional group.

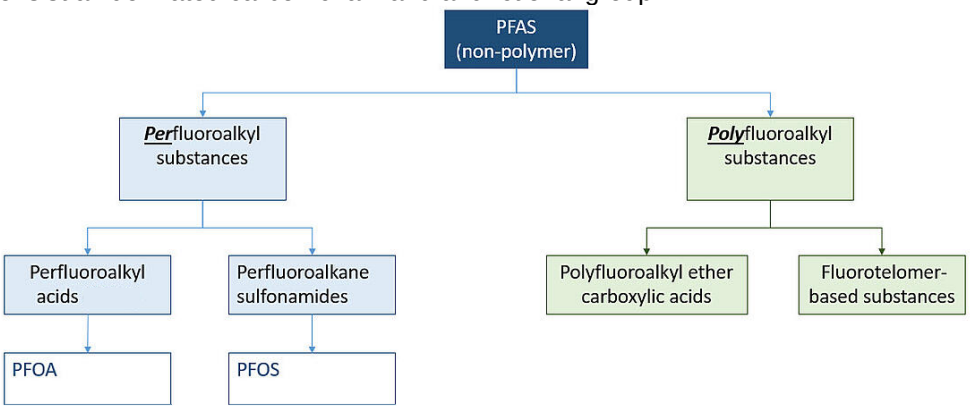

Figure 2. Simplified overview of PFAS family (edited, from https://www.bbjgroup.com/pfas-everything-you-need-to-know)

Both PFOA and PFOS are in the perfluoroalkyl group. Compared to other less used PFAS, PFOA and PFOS have been studied much more.

PFOS is a member of the perfluorosulfonic acid group (PFSA). PFSA substances have a chain of fully fluorinated carbon atoms, as depicted in Figure 1. Their functional group is a sulphate molecule at the head of the carbon chain. The carbon chain varies in length from 2 to 16 carbon atoms.

The length of the chain is represented in the name for instance in PFOS which stands for perfluorooctanesulfonic acid, which contains the word octane, indicating 8 carbon atoms in the chain.

Like PFSA, perfluorinated carboxylic acid substances (PFCA) have a carbon chain of 2-16 carbon atoms in length. The functional group is a carbonic acid at the head of the carbon chain. PFOA is the most well-known substance in this group and is often called C8, again after the length of the carbon chain. The difference with PFOS is that PFOA has the 8th C atom in its functional group instead of in the carbon chain, see Table 1.

Notable to mention is the existence of precursors. A precursor is not a type of PFAS, but a PFAS molecule that has the potential to form a PFSA or PFCA. They are larger PFAS molecules that can end up in the environment and can be degraded by natural processes into PFSA or PFCA, for instance PFOS and PFOA. Degradation of precursors in the soil is an aerobic process (Rigét et al., 2013). Only the non-fluorinated parts of the precursor molecule are broken down (Pancras et al., 2018). PFOS and PFOA do not degrade naturally.

2.1.2 Physicochemical properties

Although PFOS and PFOA have been researched extensively compared to other PFAS, physical and chemical data is still relatively scarce and their behaviour in soils is not well understood. The following table presents some physicochemical properties that are relevant for their fate in the environment.

Table 1. Physicochemical properties PFOS and PFOA after Pancras et al. (2018). In the chemical structure figures, C atoms are found at every intersection point of multiple lines. The 8th C atoms in PFOA is in the functional group.

Properties	PFOA	PFOS
Melting point	54-55°C	54°C
Boiling point	189-192°C	>400°C
Vapor pressure	4-1300 Pa (at 25°C)	6.7 Pa (20°C)
Henry Constant	0.04-0.09 Pa·m^3·mol^{-1}	2e-6 - 3e-4 Pa·m^3·mol^{-1}
Solubility in (pure) water	9500 mg/L	550-570 mg/L
Physical state at 25°C	White powder/waxy solid	White powder
Chemical structure	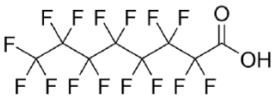	

Three properties are relevant for the transport of PFAS in the atmosphere and soil:

1. Vapor pressure (Pa)

PFAS have a very low volatility. The only exception are fluorotelomer alcohols, a type of polymer that has a relatively high volatility compared to the other PFAS. This means that most PFAS barely evaporate once they accumulate in the environment.

2. Henry constant (K_H)

The Henry constant describes the distribution of a substance over the liquid and gas phase at a certain temperature. PFOA has a Henry constant similar to benzene. Wang et al. (2011) found that most PFAS dissociate in water into a cation or anion. Their affinity with the water phase is therefore stronger than with air, which makes them less volatile than expected based on their physical properties (Prevedorous et al., 2006). Thus, volatilization is an insignificant transport mechanism. PFOS has an even lower Henry constant so also for this substance volatilization is a negligible transport mechanism.

3. Partition coefficient (K_{oc}).

The normalised organic carbon to water partition coefficient is a measure of sorption that relates the organic carbon (OC) content in a soil to the sorption coefficient, K_d. The K_{oc} value can be determined under lab- or field conditions and is different for different PFAS (Concawe, 2016). In literature it is often written in log-form. Some of the often cited sources and their K_{oc} values are listed in Table 2. Because the range in K_{oc} is large, the range of K_d is also large. More about the relation of OC to K_{oc} and K_d is described in Chapter 3.4.2.

Table 2. Log K_{oc} and the literary source.

Source	PFOS Log K_{oc} [L/kg]	PFOA Log K_{oc} [L/kg]
Concawe (2016)	2.5 - 3.1	1.3 - 2.35
Higgins & Luthy (2006)	2.57	2.06
3M Co. (2000)	2.57-3.1	-
DuPont (2003)	-	1.9-2.17
Weber et al. (2017)	3.37	2.61
Milinovic (2015)	2.85	1.98
Nguyen et al. (2020)	2.7-3.5	1.8-2.7

A PFAS molecule often has a hydrophobic tail (the C chain) and hydrophilic head (functional group such as sulfonate). This makes them ideal as surface-active substances, often called surfactants. PFAS lower the surface tension between liquid-liquid, liquid-gas or liquid-solid phases. What make PFAS more unique than other surface-active substances, is that the tail also has lipophobic properties which makes them water *and* fat repellent. They can be used to mix two unmixable liquids (water and oil) but also to protect surfaces from water and oil, acting as a repellent coating. More conventional surface-active substances often lack this lipophobic property (Pancras et al., 2018).

2.2 Production and application of PFAS

Production of PFAS happens by electrochemical fluoridation (ECF) and teleomerisation (TM) (Pancras et al., 2018). Nowadays, TM is the most applicable technique as it results in a more pure product. The most well-known production locations in Europe are the 3M locations in Zwijndrecht (Belgium) and Miteni (Italy). The surrounding areas of these locations have been polluted because of (licensed) emission of PFAS (Pancras et al., 2018). The 8 largest producers and users of PFAS in Europe (Arkema, Asahi, BASF, Clariant, Daikin, 3M/Dyneon, Dupont and Solvay Solexis) have stopped using PFAS as of 2015 (Pancras et al., 2018).

In the Netherlands, no production of PFAS has taken place but PFAS has been used in the production of polymers in the Chemours factory in Dordrecht. From 1970 till 2012, PFOA was used for production of Teflon, fluorinated ethylene propylene (FEP) and Viton (a specific rubber) (Pancras et al., 2018). From 2013 and onwards, the factory has replaced PFOA for Gen-X, a substitute chemical with similar properties and behaviour. The emission of PFOA into the air and surface water was licensed. In the 1990's, 10,000 to 13,000 kg of PFOA was disposed of annually in the Beneden Merwede River (Tweede Kamer, 2017). The emission into the air was in the order of 5,000 kg/year (Koch et al., 2017).

The application of PFAS is manifold. Examples are water and oil repellents for leather, paper and textile, chroming plating, waxes, cleaning detergents, ink, cosmetics, fire extinguishing foams, lubricants and varnishes (Paul et al., 2009).

Regulation of use
Currently the production and use of PFOS and PFOA is limited because they have been added to the REACH regulation and the Treaty of Stockholm (Pancras et al., 2018). An international group of 200 scientists has requested to reduce the use of PFAS and to develop alternatives (Madrid statement, 2015; Helsingør statement, 2014). PFOS was added to the REACH regulation and Treaty of Stockholm in 2009 as an Persistent Organic Pollutant. Since July 2020, PFOA is not allowed to be traded in the EU. It is not allowed to produce a mixture, substance or object with more than 25 parts per billion PFOA.

The Netherlands and four other northern European countries (Denmark, Germany, Norway and Sweden) are currently working on a European ban on PFAS. The restriction will apply to the whole family of PFAS, to avoid endless replacement of PFAS variations. The restriction would ban the whole group of PFAS in Europe, including import of products containing PFAS. The proposal is currently in the first phase of the process toward a decision of the European Chemical Agency (RIVM, 2020).

2.3 Environmental fate

The occurrence, transport and toxicity of PFAS in the environment are described in the following paragraphs.

Occurrence
PFAS are not naturally occurring, yet PFAS are even found in polar bears on the North Pole (Pancras et al., 2018). The three properties highlighted in Chapter 2.1.2 cause them to travel far by route of air and water. The C-F bond is very rare to encounter in natural substances and is one of the strongest connections in organic chemistry (Pancras et al., 2018). The fluorine atoms shield the PFAS molecule from heat, acid, photolytic radiation and chemical weathering.

PFOS is used as non-dissociated acid or as a salt (often containing ammonium, kalium or lithium) (Pancras et al., 2018). It is the most found type of Perfluoroalkyl in the environment and in the liver of wild animals (Giesy et al., 2010).
PFOA is also used as non-dissociated acid or as carbonic acid anion. In water, both are found as carbonic acid anion. Under natural circumstances and pH levels (5-9) both PFOA and PFOS are found as anion in soil and groundwater (Pancras et al., 2018).

Transport
PFAS mainly enter the environment via two routes, either by transport via the air (followed by deposition) or by transport in ground-, surface- and seawater (Rigét et al., 2013). They can be emitted in the production process and attach to aerosols which then rain out (Zeilmaker et al., 2016). Figure 3 is a simplified sketch of how the transport via air occurs.

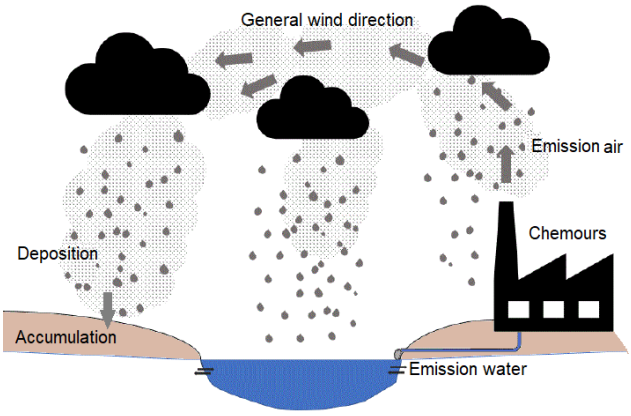

Figure 3. PFAS ways of transport (modified from van Bentum et al. 2017).

In this research, the emission route through air is relevant as only the content-depth profiles of PFAS in undisturbed soils, far from the Merwede River, are studied. Once PFAS have been deposited on the soil, transport with water becomes relevant. As mentioned earlier, PFOS and PFOA are found as anion. Because soil components and especially clays are in general slightly negatively charged, both substances do not adsorb well onto clay particles (Li et al., 2012). Organic matter (OM) content is an important factor with regard to PFAS sorption and transport in soils.

Higgins and Luthy (2006) found that PFOS has a stronger bond to OM than PFOA. Because their hydrophobic tail and hydrophilic head, PFAS tend to accumulate at air-water interfaces. Their behaviour is comparable to soap and they can also form micelles. Normally, the K_{ow} (octanol-water) is used to predict adsorption of the pollutant to soil. In the case of PFAS, this is not applicable, because the K_{ow} is often not measurable due to the lipophobic and hydrophobic properties (Pancras et al., 2018). K_{oc} is used more frequently as sorption parameter in PFAS studies.

2.4 Toxicity

Toxicity is an important aspect for human health and the environment. Exposure of PFAS to people mainly occurs through drinking water or food. It is not so much acute toxicity, but long term exposure increases the risk of liver failure, long failure, disruption of hormone levels, reproduction malfunction and growing disorders (Kristensen et al., 2013). There is a strong link between exposure to PFAS and several types of cancer (Mastrantonio, 2017).
The tolerable daily intake (TDI) for PFOA was determined by the RIVM in 2016 to be 12.5 ng/kg body weight per day. It was not determined for PFOS. The 2016 standard formed the basis for policy. The European Food Safety Authority (EFSA) recently set a new threshold for safe intake of PFAS (EFSA, 2018). They used a definition of tolerable weekly intake (TWI) which is as follows:

- 4.4 ng/kg bodyweight for PFAS in general
- 13 ng/kg bodyweight for PFOS
- 6 ng/kg bodyweight for PFOA

This is a lot less compared to their earlier study (EFSA, 2008) when the tolerable TDI was 150 ng/kg bodyweight for PFOS and 1500 ng/kg bodyweight for PFOA. The 2018 EFSA report resulted in discussion at the RIVM, because the TDI was 15 times stricter than the TDI that was set by the RIVM in 2016. The RIVM is currently reviewing the new standard by the EFSA and will likely follow the conclusion of that report, lowering the threshold value of TDI for PFOA and PFOS.
Risk level threshold values have been set for different environmental compartments. For soils, groundwater and surface water an intervention value was determined. This values gives the scientifically determined norm for the quantity of the substance at maximum allowed risk level. The background value is a content that is desired as natural standard. Research by Moermond et al. (2010), Lijzen et al. (2018) and Wintersen et al. (2016) has led to the quantification of the threshold values, see Table 3.

Table 3. Environmental standards as derived from Moermond et al. (2010), Lijzen et al. (2018) and Wintersen et al. (2016) in µg/kg dry soil.

	Class	PFOS	PFOA
Soil	Intervention value	6600	900
	Background value	1.4	1.9
	Intervention value garden	6600	900
	Living with vegetable garden	-	86
Water	Intervention value groundwater.	4.7 µg/L	0.39 µg/L
	Target value groundwater	0.23×10^{-3} µg/L	-
	Surface water	0.65×10^{-3} µg/L	0.048 µg/L

3 Materials and Methods

The research project comprised of field work, laboratory work, data collection and hydrological transport modelling. The methods employed for these activities are described below.

3.1 Data collection

Prior to the fieldwork, analysis and transport modelling, a literature review was conducted (Chapter 2). Important sources that were consulted are the websites of the RIVM and Expertisecentrum PFAS that have published PFAS research in the Netherlands and more specifically about PFOA in relation to Chemours. To obtain a more complete overview of relevant publications, queries were made using Google Scholar and Google search. The information that was collected from literature sources was used to write the background chapter and to collect physical soil- and substance parameters that were used as input for the hydrological model. The results that followed from the fieldwork, laboratory analysis and transport modelling were compared to existing studies on PFAS transport in soils where relevant.

3.2 Fieldwork

Fieldwork was done to collect soil samples that were analysed for PFOA and PFOS content, organic matter content and grain size.

Four drillings where made at four locations within 50 km of the Chemours factory, see Figure 4 on page 21. In total, 40 soil samples were collected. The drilling locations were identified based on the following criteria:

1. Downwind of Chemours, so in predominantly N-NE direction considering the prevailing S-SW wind direction.

2. Vertical infiltration of precipitation and absence of seepage.

This requirement was formulated to ensure that the vertical profile represents actual historical transport downward and to be able to use a one-dimensional (vertical) transport model for the transport modelling (Chapter 3.4).

3. Homogeneous soil, either sand or peat.

This was necessary to intercompare mobility in two completely different soils.

4. Not disturbed, i.e., no ploughing or so, in the past 50 years.

Undisturbed topsoil in natural or agricultural areas was a prerequisite so that the PFAS content in samples can be linked to historical emission and deposition. In disturbed or ploughed soils, the content-depth profile does not serve as a historical archive due to mixing. In urbanized areas, other sources of PFAS may play a role. Samples were taken with a short depth interval to gather detailed data on vertical variation of soil properties and PFAS content.

Based on the hypotheses (Chapter 1.3), the first 100 cm were sampled with a higher interval (every 10-20 cm) followed by a coarser interval (every 50-100 cm) down to the depth of the groundwater table in the sandy soils. This was done because exact groundwater levels and their temporal fluctuations were unknown and most variation in PFAS content was expected in the first 100 cm. At the site containing peat, samples were taken down to a depth of 140 cm which was below the groundwater table. In total, 104 samples were taken. Out of these 104 samples, 40 were selected to be analysed in the University- and TNO laboratories. Table 4 shows the location, sample depth and numbers of samples that were taken per location.
At every depth interval, two samples were collected. One sample for analysis of PFAS and one for thermographimetric (TGA), CS-elemental and grain size analysis (see Chapter 3.3 for further explanation of these methods). The samples for PFAS were taken with an apple corer that was cleaned with methanol before use. The samples for TGA, CS elemental, and grain size analyses were taken with a metal spoon and put in sample jars. The sample jars that were used to collect PFAS sample were pre-cleaned with methanol to minimize possibility of PFAS pollution from other sources than the sample. Prior to the fieldwork, materials had to be ordered, gathered and cleaned. A list of used materials is added to this report (Appendix A).

Table 4. Overview of sampling locations and the samples taken for laboratory analysis.

Location	Abbreviation	Coordinates (RD)	Number of samples	Sample depths below surface in cm.
Schoonenburgsche heuvel	SH	109329, 433336	12	10, 20, 30, 40, 50, 60, 70, 100, 150, 220, 300, 350
Schoonenburgsche heuvel peat	SHP	109310, 433220	8	10, 30, 50, 70, 90, 110, 130, 140
De Donk	DD	113671, 434004	8	10, 20, 40, 60, 80, 120, 200, 300
Hoornaar	HO	124202, 433004	12	5, 10, 20, 30, 40 50, 60, 70, 100, 150, 200, 250.

3.2.1 Locations

Based on the four criteria, inland dunes that are present in the riverine part of the Central Netherlands were the preferred locations. These dunes are composed of aeolian sand and occur as local outcrops called in the landscape having an altitude several meters above their surroundings. They are called ‘donk’ in Dutch so the name of one of the sampling sites directly refers to the geomorphological feature. The groundwater level is relatively deep at these geomorphological features and infiltration of rain water is typically vertical. The exact sites were further identified using Google Earth, Dinoloket, Topotijdreis and AHN. Based on these sources, three sites contained sandy soils and the fourth contained peat soil. An exploratory visit was made to the locations to ask for permission as all locations are on private land.

Out of the four selected locations, three were taken on sandy inland dunes and one in a peat grassland. The first drilling was made at the Schoonenburgsche heuvel which is at the top about 5 m higher than the surrounding grassland. Based on the data of BRO GeoTOP, it was likely to find a homogenous sand layer of at least one meter thick on this hill. It was chosen to make a drilling on the windward side, close to the top of the hill. The second drilling was made in the peat land on the windward side, about 100 m from the borehole on the Schoonenburgsche heuvel. The third location was in the backyard of a resident of a hamlet called De Donk. De Donk is a hill very similar in height and size to the Schoonenburgsche heuvel, except that De Donk has been inhabited for the past 200 years. According to the landowner, the soil was undisturbed for at least 30 years. The fourth location was chosen on the windward side of the main road in Hoornaar in a grass field. The village of Hoornaar is built upon an elongated donk. Same as for De Donk and the Schoonenburgse heuvel, this location was chosen for its relative high altitude compared to the peat landscape surrounding the donks.

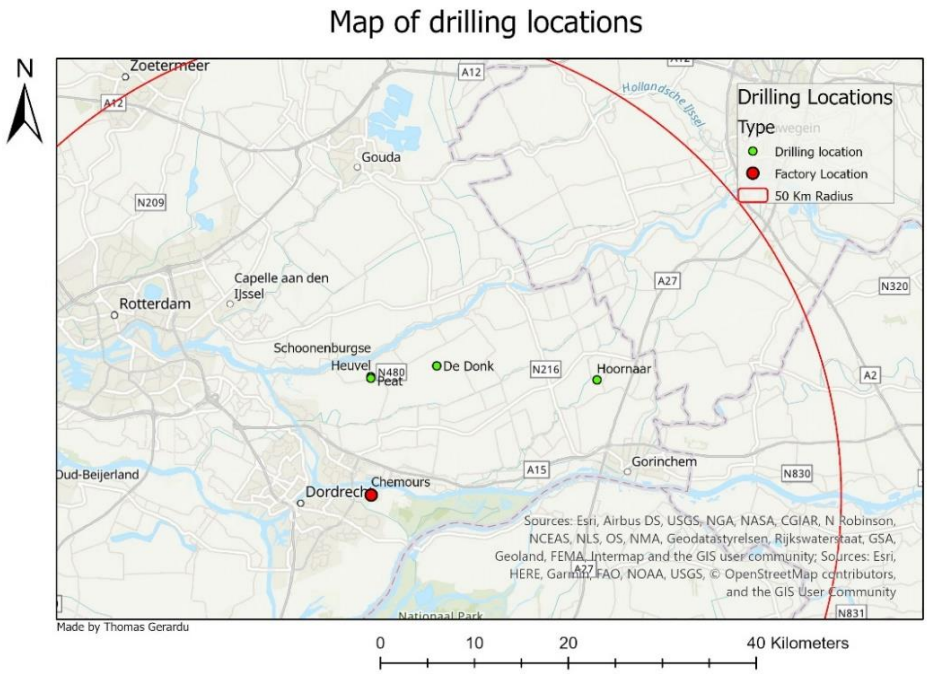

Figure 4. The Chemours factory and the four drilling locations. Note that Schoonenburgsche heuvel and Peat are very close to each other.

3.3 Soil physical and chemical analysis

Four types of sediment analyses were performed: thermogravimetric analysis (TGA), carbon-sulphur (CS) elemental analysis, grain size analysis and Liquid Chromatography combined with Mass Spectrometry (LC-MS) analysis. The LC-MS analysis was done to determine the content of PFAS in the soil samples.

3.3.1 Organic Carbon

Organic carbon can be determined via multiple ways, among which TGA and CS elemental analysis. The organic matter content (OM) was determined with TGA. The organic carbon content (OC) was determined with CS elemental analysis.

The combined results were used to calculate the organic carbon component in the soil samples. Organic carbon was used to calculate the sorption parameter K_d (Chapter 3.4.2). OM is related to OC by a conversion factor. The conversion factor was derived by plotting all OC values of the CS elemental analysis against the OM values determined with TGA. A trendline was added to the OC/OM graph. The slope of the trendline was used to find the conversion factor to convert OM to the fraction of organic carbon, f_{oc}.

Thermogravimetric analysis.
TGA is a method used in soil analysis to determine (among others things) the fraction of organic matter of a given soil sample. The analysis was carried out by a Utrecht University professional who did the following: the 40 soil samples were placed on a scale and weighed at the start of the analysis. During the analysis, the temperature increased gradually from 25°C to 1000°C over a pre-set time. Samples were first heated from 25°C to 105°C after which the temperature stabilized for 3.5 hours. This was done to evaporate all residual moisture from the initial soil sample. Then the temperature was linearly increased from 105°C to 1000°C over 13 (± 1) hours. The weight loss between certain temperature intervals was assigned to loss of a certain soil compound, such as organic carbon. The range 110-450°C is the typical temperature range where all organic carbon is completely oxidised (Roskam, Klaver and Griffioen, 2008). The mass loss in the range 450-550°C is predominantly caused by the inorganic fractions like ferrous carbonate and siderite (Roskam et al., 2008). Calcium carbonate ($CaCO_3$) starts to decompose above 600°C (Kasozi, Nkedi-Kizza & Harris, 2009) up to about 800°C (Roskam et al. 2008). The range 550-700°C may also be governed by mass loss from montmorillonite and pyrite.

Pallasser et al. (2013) and Laird et al. (2008) state that TGA can be used to both broadly distinguish between carbon forms in samples and as a quantitative analysis. The method is best applicable to sandy or peaty soils and is less accurate for clayey soils (Heiri, Lotter & Lemcke, 2001). TGA chosen because it is a relatively easy and fast method to determine organic matter. The output of this analysis method is a spreadsheet with sample name [-], time [s], weight [g] and weight loss [%]. These can be used to calculate the organic matter as fraction of the initial sample as:

$$OM[-] = \frac{OM\ [g]}{Dry\ Soil\ [g]} \quad (1$$

Carbon-sulphur elemental analysis.
CS elemental analysis is done to determine the fraction of carbon and sulphur in a given sample. A soil sample is brought into a furnace that is heated to the point where the carbon and sulphur atoms form gasses, predominantly CO_2 and SO_2. SO_2 is measured by leading the gas through a channel with an ultraviolet light. Sulphur dioxide absorbs the light and the decrease in light intensity is a measure of the amount of SO_2 in the gas, which can be related to amount of sulphur in the sample. The same principle applies to CO_2, but instead infrared light is used.
For this research, the Leco SC-632 was used which has a detection limit of 0.1% for carbon and 0039% for sulphur. The measuring accuracy is 0.039% for carbon and 0.013% for sulphur.

The analysis was carried out by a Utrecht University professional who followed the procedure described in ISE report 2001 and ISE Report quarterly report 99.2. CS elemental analysis was chosen because it is an often used technique to determine total carbon or OC. The output is a spreadsheet with sample name [-] and OC as weight fraction of the dry sample [%]. The results regarding the sulphur analysis did not have to be used.

3.3.2 Grain size analysis.

Grain sizes was determined using a Malvern Mastersizer. The samples were inserted in the instrument in a compartment of demineralised water. The blender speed was set to 2000 rotations per minute (empirically determined). A certain sample quantity was needed before the measuring procedure could be started. This method was chosen because it gives very accurate results of grain sizes (0.02 µm). The analyses were used to determine texture classes and calculate hydraulic conductivity (K_s) of the soil (Chapter 3.4.2). The texture classes are based on the US Geological Survey (USGS) classification system.

3.3.3 PFOA and PFOS analysis.

PFOA and PFOS were analysed by making use of the TNO facilities in the laboratory. Pre-treatment consisted of the following steps: first, the samples were spiked with an internal standard and dried for 48 hours. The internal standard was added for reference. Ideally, 100% of the internal standard is found in the LC-MS but this is almost never the case. The assumption is that whatever amount of sample is lost in the preparation stage, the same proportion of extract is lost in the sample. Then, 2 grams of dried sample needed to be transferred to 15 ml PP vials where 2 extraction steps were taken to extract as much PFAS molecules from the soil into the extract as possible. Then the extract was applied on an SPE column to concentrate all the PFAS molecules on the sorption medium. Next, the columns were eluted and the elution was dried. Lastly, methanol was added to the dried extract in the vial to dissolve all the concentrated extract which was then inserted in 0.3ml insert vials that were analysed with LC-MS. The TNO protocol can be accessed on request.

The pre-treatment method has been used prior to this research and was proven to be accurate while some samples have been analysed in triplicate to verify whether this was still the case. The output is a list of samples and their PFOA and PFOS content in microgram per kilogram dry soil. The detection limit was 0.05 µg/kg dry soil.

3.4 Transport modelling

The model code HYDRUS was used to model reactive transport of PFAS in the unsaturated zone. In this research, use is made of a water and solute transport model. According to a AECOM (2020), HYDRUS was the best available option of the reviewed vadose zone models. Modelling PFAS transport with solute transport models is a relatively new field of research. Attempts to model transport with (modified) HYDRUS-1D are recent (Costanza-Robinson et al., 2017; Silva et al., 2019.). During this research, a relevant article was published by Silva et al. (2020) who modified the HYDRUS script to simulate PFAS transport in the vadose zone. Co-author and founder of the HYDRUS software J.Šimůnek was contacted to ask about the availability of this new modification for public use but due to property rights and funding, the new modification is not yet released. Instead, use was made of the newest publicly available version of HYDRUS-1D (4.17.0140 last updated in 2018). The suffix indicates 1-dimensional transport of water and solutes. Minor importance is given to the hydrological theory on which the model is based, except for when this is needed to explain choices in model set-up or when elaboration is needed to analyse model results.

3.4.1 General model set up

Model scenarios had to be made in HYDRUS to model the transport of water and solutes. The model consist of 14 pre-processing steps that need to be specified in order to run the model. In these steps one can make a model version of the reality using parameters that describe soil, water and solute properties. The parameters used are listed in Table 5. The scenario was as follows: the four locations have been exposed to PFAS deposition between 1970-2012. The PFAS contamination originates from wet and dry atmospheric deposition. There are four soil columns (unsaturated) that received precipitation with a certain concentration of PFAS for 42 years. The next paragraphs describes the parametrisation and pre-processing steps in more detail.

3.4.2 Parametrisation

The input parameters that were used are listed in the following table including how this parameter was determined. When the source is ‘default’ this means that the parameter is taken from the standard value in the model (e.g. when one chooses ‘sand’ or ‘loam’ as texture class, the model automatically assigns water flow parameters for this soil type). The HYDRUS program is equipped with a standard set of empirically determined parameters for different soils and solutes based on van Genuchten (1980), Carsel and Parrish (1986) and Schaap et al. (2001).

Table 5. Model parameters and how established. Length units are abbreviated as L, time as T, mass as M and volume as V. Blue tint indicates water flow parameters, brown tint soil and solute parameters.

Nr#	Parameter	Symbol	Unit	Source
1	Depth of soil profile	-	L	Borehole data
2	Residual soil water content	θ_r	Fraction	Default
3	Saturated soil water content	θ_s	Fraction	Literature
4	Parameter α in the soil water retention function	-	L	Default
5	Parameter *n* in the soil water retention function	-	-	Default
6	Saturated hydraulic conductivity	K_s	L/T	Analysis + Literature
7	Tortuosity parameter in the conductivity function	T	-	Default
8	Bulk density	ρ	M/V	Analysis + Literature
9	Dispersion Coefficient	D_L	L	Literature
10	Fraction of adsorption	-	Fraction	Default
11	Molecular diffusion coefficient in free water	D_w	L	Literature
12	Adsorption coefficient	K_d	L^3/M	Analysis + Literature
13	Adsorption isotherm coefficient 1 (Langmuir)	η	L^3/M	Default
14	Adsorption isotherm coefficient 2(Freundlich)	β	-	Default
15	Solute concentration of incoming water	-	M/V	PFAS Profiles

The depth of the soil profiles was taken as the distance from ground level to the water table at each location. The values for K_s, ρ, K_d where based on the results of the fieldwork, TGA, CS elemental and grain size analysis. The bulk density (ρ) was not directly measured with the grain size analysis but the results of the analysis were used to determine the texture class, based on d50 value. De Vries (1999) was consulted to look up bulk densities with the corresponding texture classes. The K_s and K_d were based on two relationships described in the next section. The concentration of PFOA and PFOS in the precipitation was calculated from the PFAS profiles. More about this parameter is explained in Chapter 3.4.2.3.

For saturated hydraulic conductivity, the following equation was used (Hazen 1982).

$$K_s = C_H \frac{g}{v} d_{10}^2 \quad (2$$

Where K_s is saturated hydraulic conductivity [m/s], C_H is a unitless coefficient of $6.54 \cdot 10^{-4}$ (Harleman et al., 1963), g is the gravitational acceleration 9.81 m/s², v is the fluid kinematic viscosity of water of $0.89 \cdot 10^{-6}$ m²/s at 25°C and d_{10} is the grain size diameter where 10% of the grain size is smaller than this value in meters.

The adsorption coefficient was determined using the equation of Hamaker and Thompson (1972):

$$K_d = K_{OC} \cdot foc \quad (3$$

where K_d is the sorption coefficient [$g_{sorbent}/g_{dry\ soil}$],$K_{oc}$ is the normalised organic carbon to water partition coefficient [L/kg] and is collected from literature (Table 2), f_{oc} is organic carbon content as fraction of the sample [$g_{oc}/g_{dry\ soil}$]. The f_{oc} is determined with TGA and CS elemental (Chapter 3.3.1).

The model produces a large variety of output files. The following output files were used: concentration-depth profiles, water content-depth profiles, cumulative solute flux profiles and mass balance information. The concentration-depth profiles were converted to adsorbed content-depth profiles using formula 4:

$$S = C \cdot K_d \quad (4$$

where S is the adsorbed content (PFAS) in ng/g soil and C is the concentration of PFAS in ng/cm^3 water.

3.4.2.1 Specific profile description.

First, the main processes and geometry information were specified. 'Water flow' and 'Standard solute transport' were selected. This resulted in four depth profiles. Based on OC and K_s, the number of soil materials was specified. This is best explained by an example. If for instance 12 samples from a borehole have an OC value of ± 5% in the top 3 samples, ± 2% in the next 4 samples and ± 0.5% in the deepest 5 samples, the samples with similar OC content where grouped together to form one model layer or 'soil material'. In our example, the number of soil materials is thus three. The leading parameter for the discretisation of soil material was the K_d (which is based on OC).

Secondly, the water flow parameters were specified for each profile. For all models, the single porosity 'van Genuchten-Mualem' model was selected with no hysteresis. Hysteresis was assumed irrelevant based on the 50 year time scale of the model run, the high porosity in the peat and relatively high K_s in sandy soils. For the water flow parameters, texture classes (including the default values) were selected corresponding to the texture classes determined with the grain size analysis.
As for the water-flow boundary conditions, the following was selected:

- The upper boundary conditions was an atmospheric boundary layer that allowed ponding with a depth of 2 cm.
- The lower boundary condition was a constant head (constant water table). Because the results are viewed on a multi-year time scale, intra-annual groundwater table changes were neglected. In addition, the groundwater table in the sandy soils was 2-3 m below ground level.

Thirdly, the solute transport parameters were specified for each profile. The default time- and space weighing scheme were selected: Crank-Nicholson and Galerkin Finite Elements respectively. The equilibrium model for solute transport was selected. Tortuosity was selected with the default Millington and Quirk module.
The number of solutes was two (PFOA and PFOS) and the pulse duration (=time duration of the concentration pulse) was 50 years (from 1970-2020).
The solute *transport* parameters were selected as default with the exception of the bulk density and dispersion coefficient that were adjusted based on the grain size analysis.
The solute *reaction* parameters were specified for solute one (PFOA) and solute two (PFOS). Here, the K_d is specified for each soil material for solute one and two. Because K_d depends strongly on the variability of the K_{oc} (Table 2, Chapter 2.1.2), four model runs were performed: run one with low K_{oc} for PFOA and PFOS as obtained from literature, run two with middle K_{oc}, run three with high K_{oc} and run four with adjusted K_{oc} for the best fit. These four runs resulted in four different PFAS profiles that were compared to the measured profiles.

In other words, the simulations were compared to the measured profiles to observe whether they would show similar results to the measured profiles and what K_{oc} value results in the best fit. As for the boundary conditions:

- The upper boundary condition was a concentration flux boundary, which corresponds to a variable input concentration of PFAS in the incoming precipitation.
- The lower boundary was set as zero concentration gradient, which allows free drainage of the PFAS from the profile into the groundwater.

Next, the time variable boundary conditions were specified

3.4.2.2 Meteorological data.

In the time variable boundary conditions window, atmospheric data was specified including time [year], precipitation [cm/year], evaporation [cm/year], concentration one (PFOA) [ng/cm^3 water] and concentration two (PFOS) [ng/cm^3 water]. The first three parameters were obtained from the climate database of the KNMI. How concentration one and two were determined is explained in Chapter 3.4.2.3.
The daily precipitation/evaporation data was retrieved from the weather station in Cabauw which is located within 8-15 km from the drilling locations. The dataset was modified to get precipitation and evaporation rate in cm/year. It was assumed that the precipitation and evaporation from this weather station is representable for the precipitation and evaporation rates at the drilling locations. The elements used from this dataset were 24-hour sum of precipitation (in 0.1 mm) and reference crop evaporation (Makkink) (in 0.1 mm). Cabauw's data log starts from 1986 and runs through to 2021. Precipitation input data was needed from 1970 to 2020 for the simulation. The most long-term average year was chosen to fill in the data gap of 1970-1986 and was duplicated 16 times. This year was 1988 with 725 mm precipitation and 525 mm evaporation. It was tested whether daily or yearly precipitation data would influence the model results. It proved to have little effect, so the yearly data set was chosen as the model runs were much faster.

3.4.2.3 Matching emission history to PFAS concentration.

The concentration in the precipitation is determined based on the preliminary assumption that *the total deposition of PFOA and PFOS on each location is the same as the total quantity in the profile.* In other words, all deposited PFAS is contained in the profile. Following this assumption, the cumulative PFOA and PFOS content was calculated from the profiles. It should be noted, that the validity of this assumption can to some extent be checked based on the observed concentration-depth profile at the four locations (Chapter 4.2.2).

Each location had the same meteorological dataset for precipitation and evaporation, but with location specific PFOA and PFOS concentrations varying in time. Furthermore, the concentrations were matched to the historical emission in a proportional sense, see Figure 5 and Table 6. This means that when emission was 'high', concentrations were high and vice versa. The total PFOA/PFOS quantity (in precipitation) was kept the same but the concentration over certain time periods was adjusted to match the emission profile. Figure 5 shows the yearly emissions where emission data was available.

Table 6. Actual emission history and the proportional concentration in the precipitation, based on Koch et al., 2017.

Period	Average emission in kg/year	Concentration in precipitation
1970-1985	2500	5X
1985-1998	5000	10X
1998-2003	2500	5X
2003-2012	500	X

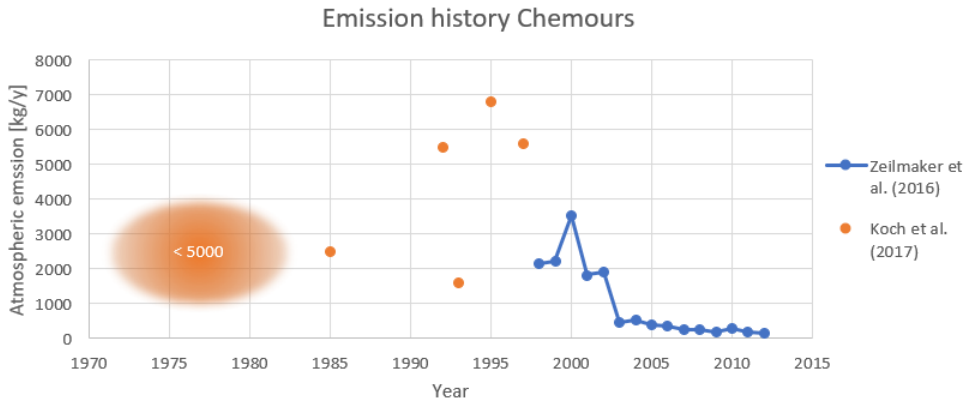

Figure 5. Emission history over time based on research by Koch et al. (2017) and Zeilmaker et al. (2016).

4 Results

The numeric results of the TGA, CS elemental analysis and LC-MS analysis are presented in Appendix B and C. This chapter presents the results as graphs or as concise tables were suitable.

4.1 Soil physical and chemical analysis

4.1.1 Organic Carbon

Organic carbon was determined with TGA and CS elemental analysis. The TGA results show that at De Donk, Hoornaar, and Schoonenburgsche heuvel, the OM content ranges between 0-6%. The deepest samples of 120 cm+ have negligible OM contents of lower than 0.3%. Overall the OM fraction decreases with increasing depth, except for two high outliers (DD-80 and HO-50 cm). The Schoonenburgsche heuvel peat samples show a contrasting pattern with 15-20% OM near the topsoil and 60-70% OM in deeper sample depths. The OM around 90, 110, and 130 cm in Schoonenburgsche heuvel peat remains more or less constant around 60%.

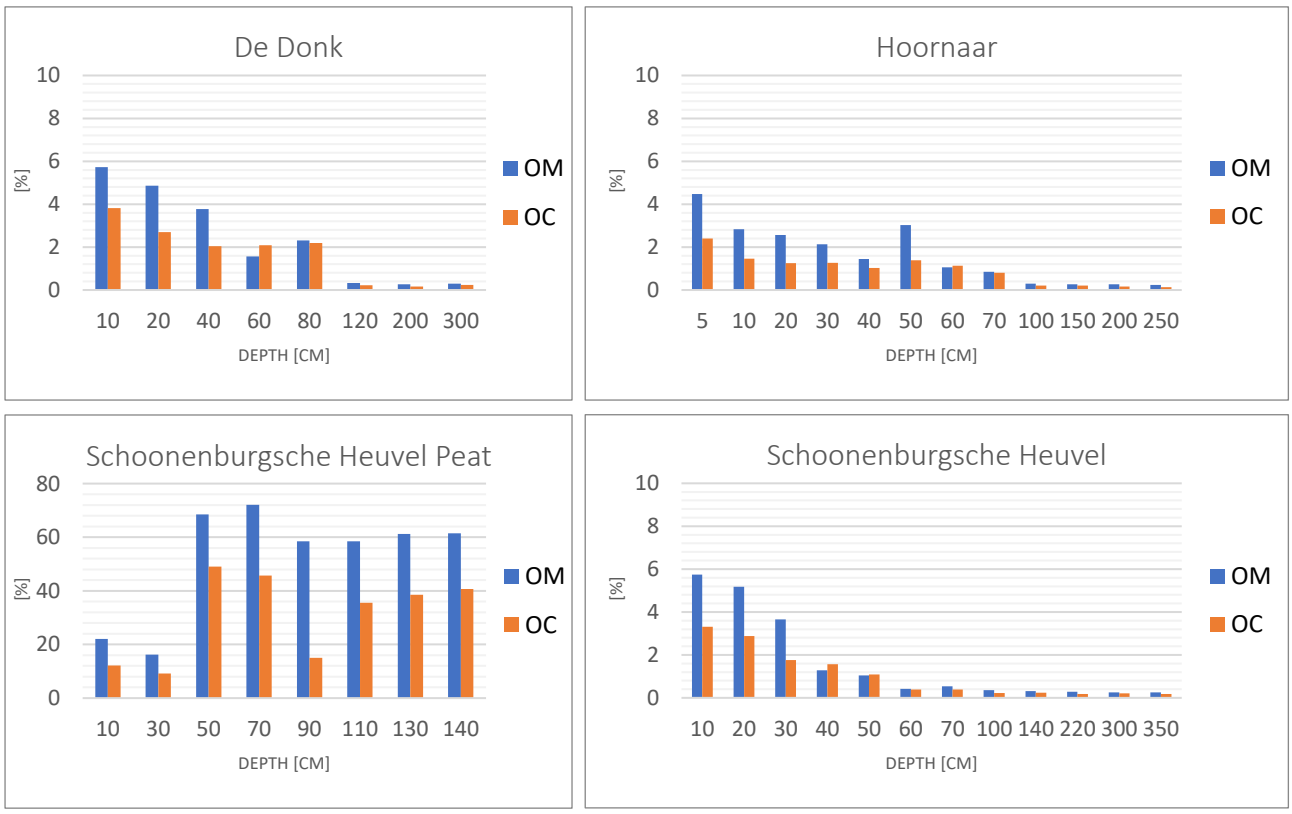

Figure 6.Organic matter as percentage of weight of dry sample. The OM is based on the mass loss between 110-450°C. The OC is determined with CS elemental analysis. Mind the different vertical scale in the lower left figure.

De Donk, Hoornaar and Schoonenburgsche heuvel show a fairly consistent pattern where the OM and OC percentages decrease gradually with increasing depth. TGA indicates that the mass loss in the range 450-700°C is small, see Appendix B. This means that the fraction of carbonate or clay minerals in the samples is very small in comparison to the OM fraction.

Schoonenburgsche heuvel peat shows a different pattern where the weight loss per temperature range is more stepwise. The upper two samples (SHP-10 and SHP-30 cm) have a much lower weight loss than at SHP-50 cm and onward. This is the result of a lower organic fraction in the soil than in SHP-50 cm and onwards. The weight loss in the range 450-550°C is significantly higher than at the other three locations (0-0.3% in samples from De Donk, Hoornaar and Schoonenburgsche heuvel compared to 3.18-5.03% in Schoonenburgsche heuvel peat). This indicates that there could be some siderite or pyrite or in the *S*choonenburgsche heuvel peat samples. The CS elemental results show a sulphur fraction of 0.02-0.03 in SHP-50 to SHP-140 cm.

The CS elemental analysis results show that the OC in samples from De Donk, Hoornaar and Schoonenburgsche heuvel is between 3.82% in the top soil and is below 1% in the deepest samples. The Schoonenburgsche heuvel peat samples shows a contrasting pattern with around 10% OC in the topsoil and 35-50% OC in deeper samples. A low outlier is observed at SHP-90 cm depth with a value of around 15%. In comparison, the OM is almost always higher than the OC, as expected. Especially with higher OM/OC values, the OC is a relatively constant proportion of OM. In samples with lower OM/OC values, the OM/OC ratio shows more deviation.

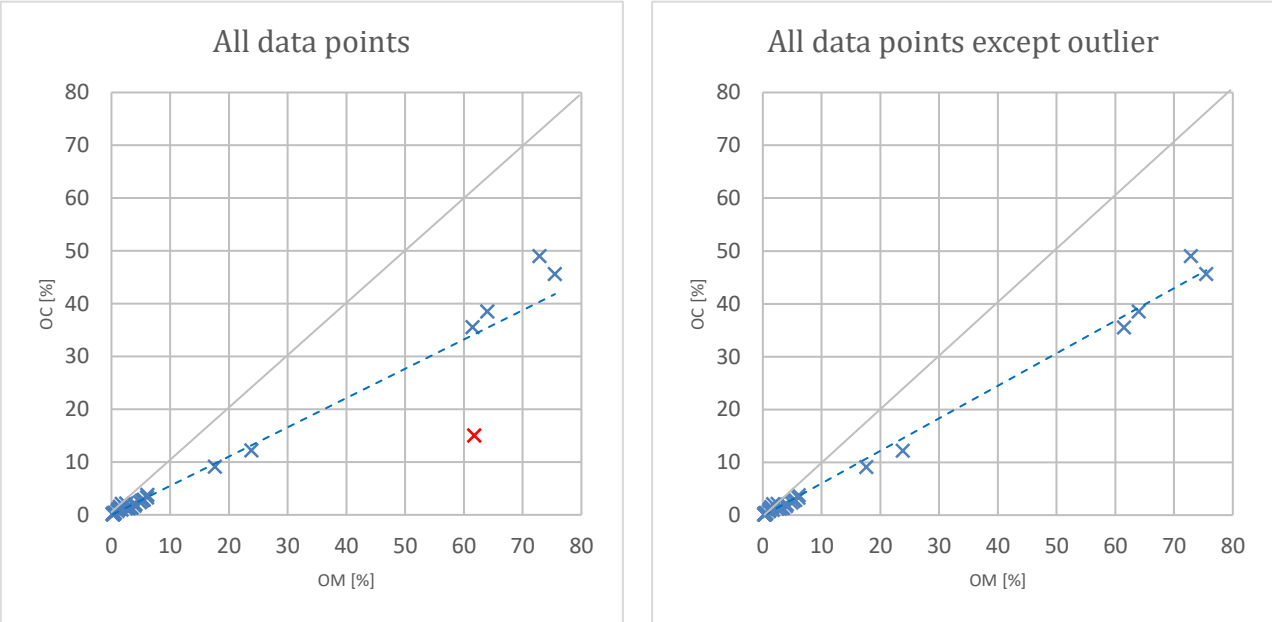

Figure 7a & 7b. The trendline for the left graph is described by y = 0,5543x-0.0444 with an R^2 = 0.924. The trendline for the right graph is described by y = 0.6157x-0.1505 with an R^2 = 0.994.

The conversion factor between OM and f_{oc} was calculated using the slope of the OC/OM graph (Figure 7) as described in Chapter 3.3.1. The outlier in Figure 7a is SHP-90 cm, which has a high OM fraction but relatively low OC fraction. This anomaly is unexplained. Using the conversion factor of 0.6157 (excluding the outlier SHP-90 cm) the following f_{oc} values are calculated (Table 7).

Table 7. OM and f_{oc} per sample as fraction.

Sample	OM	f_{oc}
DD-10	0.0613	0.0377
DD-20	0.052	0.032
DD-40	0.0408	0.0251
DD-60	0.0175	0.0108
DD-80	0.0254	0.0156
DD-120	0.0037	0.0023
DD-200	0.0029	0.0018
DD-300	0.0032	0.002

Sample	OM	f_{oc}
SHP-10	0.2384	0.1468
SHP-30	0.1761	0.1084
SHP-50	0.7287	0.4487
SHP-70	0.755	0.4649
SHP-90	0.618	0.3805
SHP-110	0.615	0.3787
SHP-130	0.6398	0.3939
SHP-140	0.6484	0.3992

Sample	OM	f_{oc}
SH-10	0.0608	0.0374
SH-20	0.0553	0.034
SH-30	0.0394	0.0243
SH-40	0.0142	0.0087
SH-50	0.0115	0.0071
SH-60	0.0046	0.0028
SH-70	0.006	0.0037
SH-100	0.004	0.0025
SH-140	0.0035	0.0022
SH-220	0.0032	0.002
SH-300	0.0028	0.0017
SH-350	0.0028	0.0017

Sample	OM	f_{oc}
HO-5	0.0488	0.03
HO-10	0.0316	0.0195
HO-20	0.029	0.0179
HO-30	0.0248	0.0153
HO-40	0.0172	0.0106
HO-50	0.0343	0.0211
HO-60	0.0128	0.0079
HO-70	0.0102	0.0063
HO-100	0.0032	0.002
HO-150	0.003	0.0018
HO-200	0.0029	0.0018
HO-250	0.0025	0.0015

4.1.2 Grain size analysis

Samples from De Donk, Hoornaar and Schoonenburgsche heuvel are predominantly classified as medium sand with a d50 ranging from 270-424 µm, see Appendix C & D. At Schoonenburgsche heuvel peat, two samples were classified as silt, one as very fine sand and five as peat (based on TGA and CS elemental analysis). No grain size could be determined for the five peat samples because they had almost no grains and the carbon content was too high for the analysis instrument. The d10 value that was used to calculate the saturated hydraulic conductivity (K_s) is displayed Appendix C. Since the d10 value of the peat samples could not be determined, de Vries (1999) was consulted for K_s values of peat in the Alblasserwaard area. The in-situ water content of the samples is presented in Appendix C.

4.1.3 PFOA and PFOS analysis

The output of the LC-MS is expressed in the form of PFAS content in microgram per kilogram dry soil for both PFOA and PFOS.

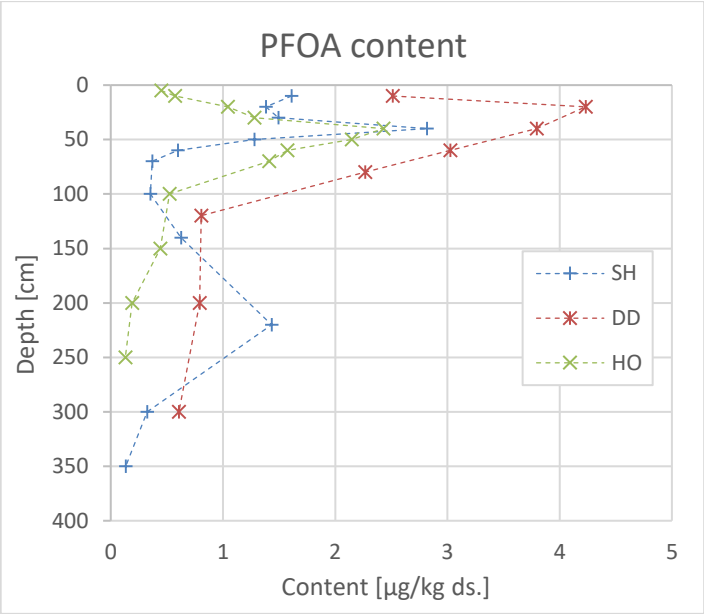

Figure 8.PFOA content in relation to depth at Schoonenburgsche heuvel, De Donk and Hoornaar.

The content of PFOA in the soil samples is in almost all sample above the detection limit (0.05 µg/kg), see Figure 8. The highest content of the samples of these three locations is at 20 cm depth at De Donk: 4.2 µg/kg. All profiles share a similar trend: PFOA content increases from ground level to about 20-50 cm depth and then decreases again with increasing depth. De Donk and Hoornaar show a similar trend from 100 cm and lower: the content slightly decrease with increasing depth. Schoonenburgsche heuvel is an exception to this trend because the content increases again, forming a second ‘peak’ at 220 cm depth. Cumulative contents for the whole soil profile at Schoonenburgsche heuvel, Hoornaar and De Donk are 4454, 2523, 6486 µg/m^2 respectively. These values lie close to each other.

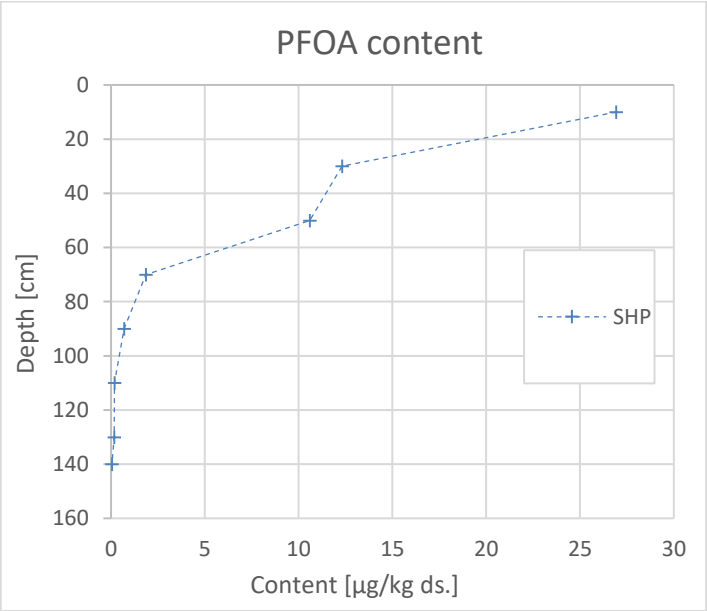

Figure 9. PFOA content in relation to depth for Schoonenburgsche heuvel peat.

Contrary to the other three profiles, the Schoonenburgsche heuvel peat profile does not have a peak in content at shallow depth but a declining content from ground level to the deepest sample (Figure 9). The contents are generally much higher than at the other three locations but the penetration depth is considerably less. The cumulative PFOA content is 4542 µg/m^2 which is very similar to the PFOA content at adjacent Schoonenburgsche heuvel (4454 µg/m^2).

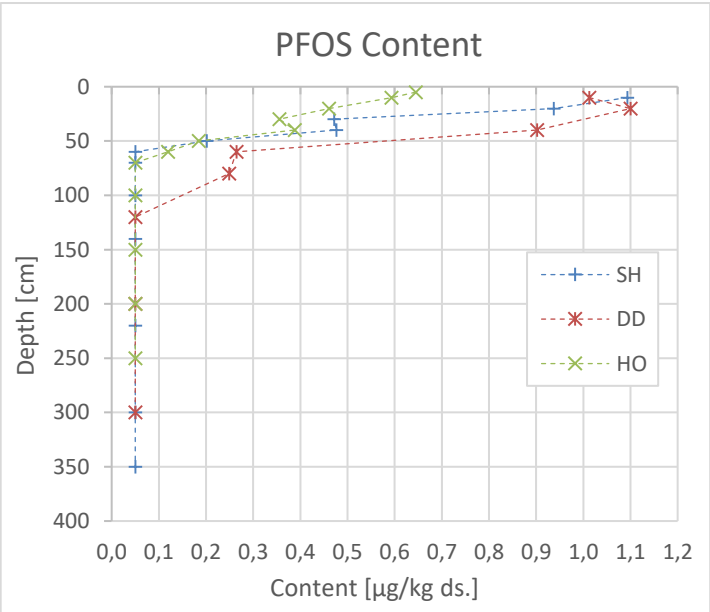

Figure 10. PFOS content in relation to depth at Schoonenburgsche heuvel, De Donk and Hoornaar.

The content of PFOS in the samples of Schoonenburgsche heuvel, De Donk and Hoornaar is lower than the PFOA content in those samples (Figure 10). Below the organic soil horizon, contents are generally below the detection limit and are plotted as having a value of 0.05 µg/kg.

There is no clear peak at some depth as is the case for PFOA. PFOS is transported less deep compared to PFOA. PFOS content in the Schoonenburgsche heuvel and Hoornaar profile decreases from top to bottom with the exception of a little plateau around 30-40 cm (Figure 10). The De Donk profile has a similar trend, but the small plateau is bit deeper (80 cm) and it is less clear. The De Donk profile also has a small peak near the top (0-20 cm domain). The cumulative PFOS contents for Schoonenburgsche heuvel, De Donk and Hoornaar are 749, 967 and 492 µg/m^2 respectively.

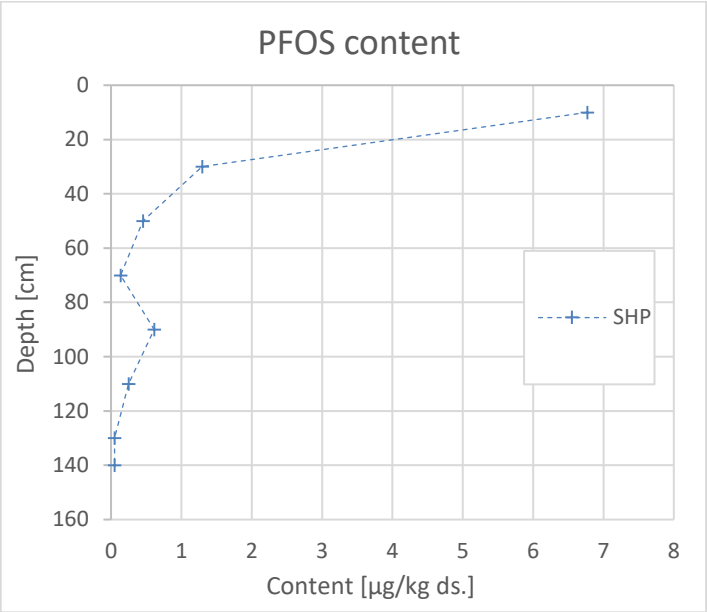

Figure 11. PFOS content in relation to depth for Schoonenburgsche heuvel peat.

The PFOS profile at Schoonenburgsche heuvel peat is very similar in shape to the PFOA profile, but with lower contents. The two lowest samples, SHP-130 and SHP-140 cm have values below the detection limit. Similar to the observation for PFOA, the contents are higher than in the other three profiles while the penetration depth is less. The cumulative PFOS content is 728 µg/m^2 which is very similar to the PFOS content at adjacent Schoonenburgsche heuvel (749 µg/m^2).

Repeatability

The analysis of PFOA and PFOS was repeated for two samples (DD-120 and SH-100 cm), in two-fold or triple-fold, to check the repeatability of the result. It was unfortunately not possible to analyse peat samples again as there was not enough sample left for second pre-treatment and analysis. The pre-treatment of samples was done following the same protocol with the exception that the internal standard was added to the sampled *after* the drying process instead of *prior to* the drying process. Table 8 shows the results of these control measurements. The second and third repetitions have similar values as the original results. The third repetition of SH-100 cm is a factor 1.58 higher than the original result. Deviations of that order need to be considered when interpreting unexpectancies or outliers in the PFOA/PFOS profiles.

Table 8. Deviation and repeatability of PFOA/PFOS in samples from De Donk and Schoonenburgsche heuvel. ‘<’ indicates below detection limit, ‘-‘ indicates not measured. Values are in µg/kg dry soil.

Location	Sample	PFOA/ PFOS	Original result	1st repetition	2nd repetition	3rd repetition
DD	DD-120	PFOA	0.81	0.78	0.72	-
DD	DD-120	PFOS	<	<	<	-
SH	SH-100	PFOA	0.35	0.30	0.31	0.49
SH	SH-100	PFOS	<	<	<	<

Cumulative content in relation to distance and wind direction.
The cumulative PFOA and PFOS contents are presented in Table 9 with the geographical distance to the source and compass direction from Chemours factory. The cumulative amounts of PFOA and PFOS in both Schoonenburgsche heuvel peat and Schoonenburgsche heuvel are very similar. Geographically they are almost the same location but the soil types are very different and so are the depth profiles. Hoornaar is further away and more eastward than the most common wind direction (SW). De Donk lies more in the general wind direction. It has a higher PFOA content and has received the most PFOA by ratio.

Table 9. Cumulative amount of PFOA and PFOS, distance to- and compass direction from Chemours.

Location	PFOA µg/m^2	PFOS µg/m^2	Ratio PFOA/PFOS	Distance to Chemours km	Direction from Chemours
SHP	4542	728	6.2	7.87	N
SH	4454	749	5.9	7.87	N
HO	2523	492	5.1	16.24	ENE
DD	6486	967	6.7	9.35	NNE

4.2 Transport modelling

4.2.1 Model input

The discretisation of the soil profile into soil layers (soil materials) with similar flow and transport parameters is presented in Tables 10-13. The exact model input of all used parameters is presented in Appendix E. This chapter focusses on the parameters K_d and K_s as they formed the distinctive criterion for layer discretization.

Note that 700 cm/d is the maximum value for K_s that is assigned to a model layer in Tables 10-13. Using equation 2, hydraulic conductivities of up to 3500 cm/day are calculated which is not deemed realistic for medium size sand. The K_s for sand was empirically determined by Carsel and Parrish (1988) to be 700 cm/d.

Table 10. Discretisation profile into layers for De Donk. The K_d [-] values result from the K_{oc} values from literature and the OC for each layer (Equation 3).

Name	K_s [cm/d]	TOC [%]	K_d (low) PFOS	K_d (mid) PFOS	K_d (high) PFOS	K_d (low) PFOA	K_d (mid) PFOA	K_d (high) PFOA	Layer nr
DD-10	105	3.77	18.9	47.5	119.4	2.4	7.5	18.9	1
DD-20	130	3.20	16.0	40.3	101.2	2.0	6.4	16.0	2
DD-40	52	2.51	12.6	31.6	79.4	1.6	5.0	12.6	3
DD-60	113	1.08	5.4	13.6	34.1	0.7	2.1	5.4	4
DD-80	39	1.56	7.8	19.7	49.5	1.0	3.1	7.8	5
DD-120	700	0.23	1.1	2.9	7.2	0.1	0.5	1.1	6
DD-200	700	0.18	0.9	2.2	5.6	0.1	0.4	0.9	6
DD-300	700	0.20	1.0	2.5	6.2	0.1	0.4	1.0	6

Table 11. Discretisation profile into layers for Hoornaar. The K_d [-] values result from the K_{oc} values from literature and the OC for each layer (Equation 3).

Name	K_s [cm/d]	TOC [%]	K_d (low) PFOS	K_d (mid) PFOS	K_d (high) PFOS	K_d (low) PFOA	K_d (mid) PFOA	K_d (high) PFOA	Layer nr
HO-05	41	3.00	15.1	37.8	95.0	1.9	6.0	15.1	1
HO-10	41	1.95	9.8	24.5	61.5	1.2	3.9	9.8	2
HO-20	46	1.79	8.9	22.5	56.5	1.1	3.6	8.9	3
HO-30	75	1.53	7.7	19.2	48.3	1.0	3.0	7.7	4
HO-40	121	1.06	5.3	13.3	33.5	0.7	2.1	5.3	5
HO-50	69	2.11	10.6	26.6	66.8	1.3	4.2	10.6	6
HO-60	700	0.79	4.0	9.9	24.9	0.5	1.6	4.0	7
HO-70	700	0.63	3.1	7.9	19.9	0.4	1.3	3.1	8
HO-100	700	0.20	1.0	2.5	6.2	0.1	0.4	1.0	9
HO-150	700	0.18	0.9	2.3	5.8	0.1	0.4	0.9	9
HO-200	700	0.18	0.9	2.2	5.6	0.1	0.4	0.9	9
HO-250	700	0.15	0.8	1.9	4.9	0.1	0.3	0.8	9

Table 12. Discretisation profile into layers for Schoonenburgche heuvel. The K_d [-] values result from the K_{oc} values from literature and the OC for each layer (Equation 3).

Name	K_s [cm/d]	TOC [%]	K_d (low) PFOS	K_d (mid) PFOS	K_d (high) PFOS	K_d (low) PFOA	K_d (mid) PFOA	K_d (high) PFOA	Layer nr
SH-10	121	3.74	18.8	47.1	118.4	2.4	7.5	18.8	1
SH-20	176	3.40	17.1	42.9	107.7	2.1	6.8	17.1	2
SH-30	145	2.43	12.2	30.5	76.7	1.5	4.8	12.2	3
SH-40	700	0.87	4.4	11.0	27.6	0.6	1.7	4.4	4
SH-50	700	0.71	3.5	8.9	22.4	0.4	1.4	3.5	5
SH-60	700	0.28	1.4	3.6	9.0	0.2	0.6	1.4	6
SH-70	700	0.37	1.9	4.7	11.7	0.2	0.7	1.9	7
SH-100	700	0.25	1.2	3.1	7.8	0.2	0.5	1.2	8
SH-140	700	0.22	1.1	2.7	6.8	0.1	0.4	1.1	9
SH-220	700	0.20	1.0	2.5	6.2	0.1	0.4	1.0	9
SH-300	700	0.17	0.9	2.2	5.5	0.1	0.3	0.9	9
SH-350	700	0.17	0.9	2.2	5.5	0.1	0.3	0.9	9

Table 13. Discretisation profile into layers for Schoonenburgsche heuvel peat. The K_d [-] values result from the K_{oc} values from literature and the OC for each layer (Equation 3).

Name	K_s [cm/d]	TOC [%]	K_d (low) PFOS	K_d (mid) PFOS	K_d (high) PFOS	K_d (low) PFOA	K_d (mid) PFOA	K_d (high) PFOA	Layer nr
SHP-10	1	14.68	73.6	184.8	464.2	9.3	29.3	73.6	1
SHP-30	1	10.84	54.3	136.5	342.9	6.8	21.6	54.3	2
SHP-50	4	44.87	224.9	564.9	1418.8	28.3	89.5	224.9	3
SHP-70	-	46.49	233.0	585.2	1470.1	29.3	92.8	233.0	4
SHP-90	-	38.05	190.7	479.0	1203.3	24.0	75.9	190.7	5
SHP-110	-	37.87	189.8	476.7	1197.5	23.9	75.6	189.8	6
SHP-130	-	39.39	197.4	495.9	1245.8	24.9	78.6	197.4	7
SHP-140	-	39.92	200.1	502.6	1262.5	25.2	79.7	200.1	7

The low, mid, high and best fit K_{oc} values are presented in Table 14. The low, mid and high K_{oc} values are collected from Nguyen et al.(2020). When 'best fit' is mentioned, the simulated content-depth profile that best matches the measured content-depth profile is meant. The best fits are obtained by scaling the mid K_{oc} value.

Table 14. Log_{10} K_{oc} value of the low, mid, high and best fit. The two shaded values are outside the low-high K_{oc} range from Nguyen et al. (2020).

	Low	Mid	High	Best fit DD	Best fit HO	Best fit SH	Best fit SHP
PFOA	1.80	2.30	2.70	2.34	2.62	2.38	2.76
PFOS	2.70	3.10	3.50	2.55	2.86	2.71	3.14

4.2.2 Model output

Firstly the model results are plotted against the measured results (Figures 12-19). There are a few general observations to be made for all the profiles:

1) The shapes of the low, mid and high K_{oc} content-depth profiles are comparable but the modelled contents are different. The high K_{oc} content-depth profile is often a magnification of mid or low K_{oc} content-depth profile. High K_{oc} results in a higher peak content and more sharp content changes as a function of depth in the profiles. The sharp changes result from the transitions between the soil layers as defined in the model. The gradual changes result from PFAS content that is different every cm.

2) The high K_{oc} content-depth profiles result in a higher content near the surface and a sharp decrease. All the PFAS is stored in the top layer(s).

3) The best fit for PFOA content-depth profiles is found with mid K_{oc} and the best fit for PFOS content-depth profiles is found using low K_{oc} values.

All figures are grouped together on pages 40 to 43.

De Donk

In the profile of De Donk the low and high K_{oc} content-depth profiles are under and overestimations of the content, respectively. The best fit is obtained using K_{oc} values within the range determined by Nguyen et al. (2020). See Figure 12.

In the PFOS content-depth profile the difference between the low and high K_d simulations is much larger. The high K_{oc} simulation overestimates the measured contents by about a factor of 5. The low K_{oc} simulation is very near the best fit simulation, see Figure 13.

Hoornaar

The PFOA high K_{oc} content-depth profile best matches the measured profile, see Figure 14. The measured profile does not decrease as sharply as the simulated profiles but has a smoother gradient.

The mid and high K_{oc} content-depth profiles of PFOS are, similar to the observation for De Donk, too high. The low K_{oc} content-depth profile fits the measured profile quite well but a slightly better fit can be achieved using the best fit K_{oc}, see Figure 15.

Schoonenburgsche heuvel

The simulations result in a slightly shallower peak content than observed for the measured profile, see Figure 16. The high value around 220 cm depth in the measured profile is not observed in the simulated profiles. This is because the simulated profiles are determined by the OC content and the OC content does not spike around 220 cm as shown in Figure 6. An adequate description is found using the mid K_{oc} content-depth profile. A slightly better fit is found using K_{oc} values a bit higher than mid-range values of Nguyen et al. (2020).

The low K_{oc} content-depth profile of PFOS results in a good description of the measured profile. The best fit content-depth profile fits slightly better (Figure 17). The mid- and high K_{oc} content-depth profiles are a factor 2 to 5 too high, respectively.

Schoonenburgsche heuvel peat

The shape of the simulated content-depth profiles is more sensitive to the chosen K_{oc} values than is the case for the three other locations. The low K_{oc} causes PFOA to become transported more downward in the profile compared to the mid- and high K_{oc} simulations. The best fit is obtained with K_{oc} values that are slightly higher than the highest threshold of K_{oc} values set by Nguyen et al. (2020). High K_{oc} causes strong sorption close to the surface whereas the peak mass has transported more downwards for the low and mid K_{oc} content-depth profiles, see Figure 18.

In the PFOS profile, the best fit is very similar to the mid K_{oc} simulation, see Figure 19. The content is much higher than at De Donk, Hoornaar and Schoonenburgsche heuvel. The simulated profiles show that most PFOS is stored in the first 20-30 cm. This is in line with the measured profile.

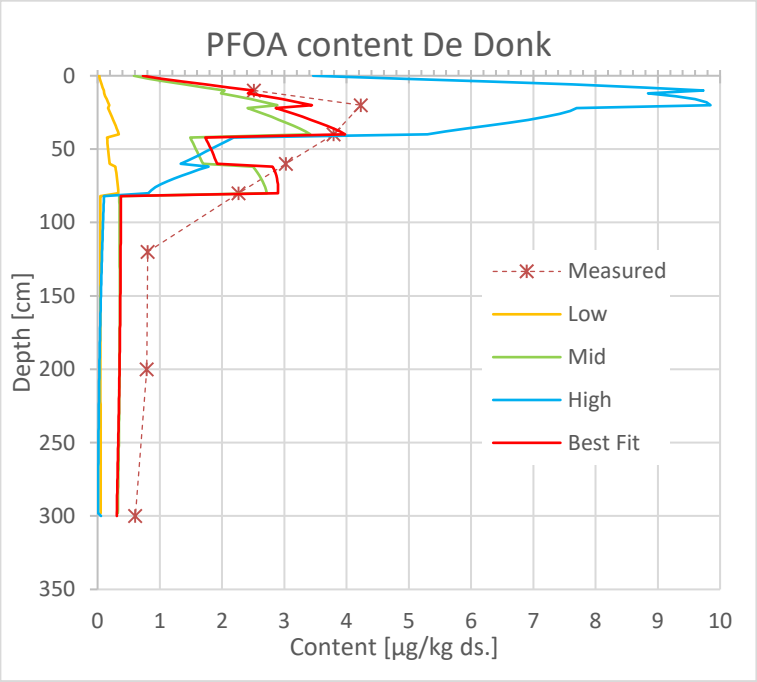

Figure 12. Measured and simulated PFOA content at De Donk.

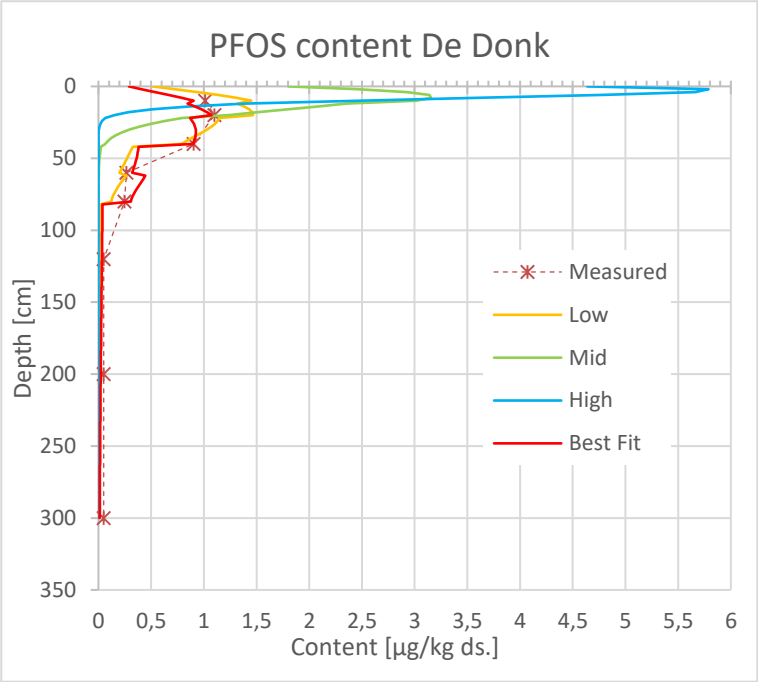

Figure 13. Measured and simulated PFOS content at De Donk.

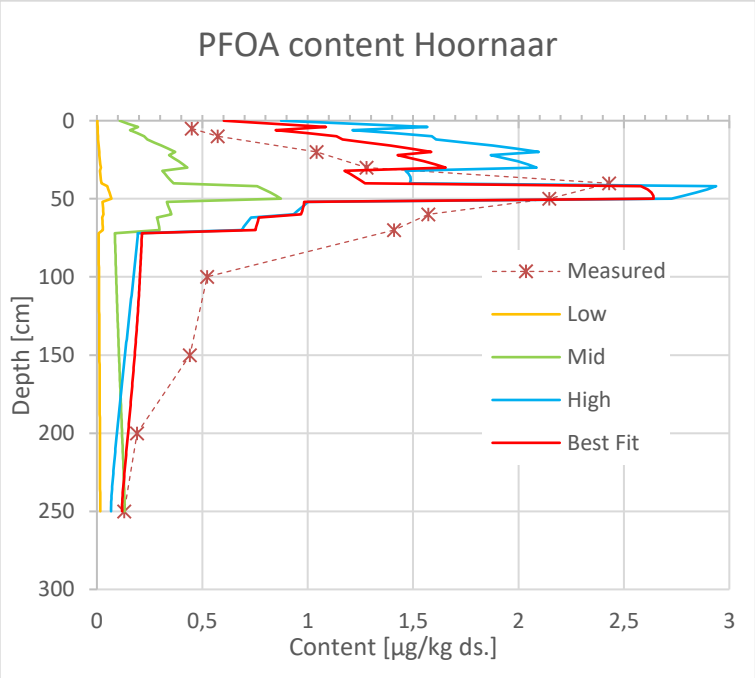

Figure 14. Measured and simulated PFOA content at Hoornaar.

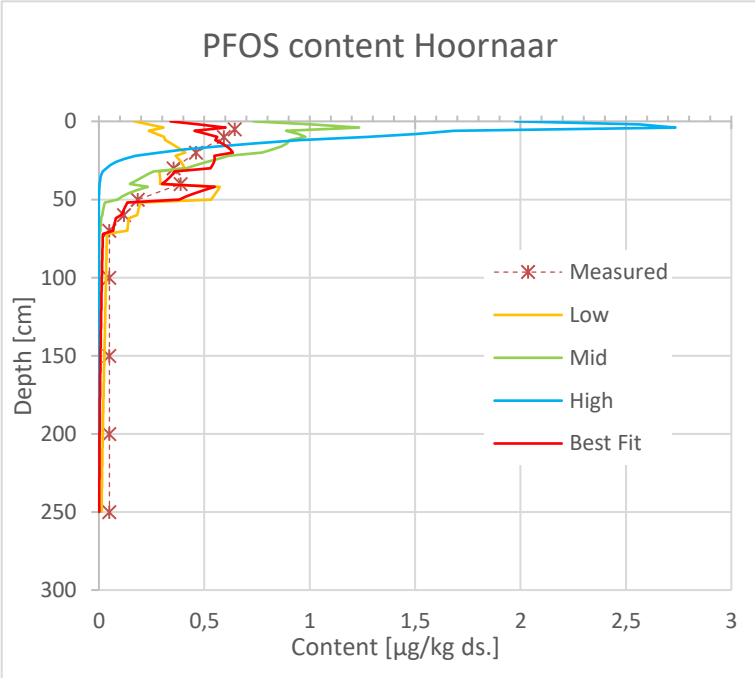

Figure 15. Measured and simulated PFOS content at Hoornaar.

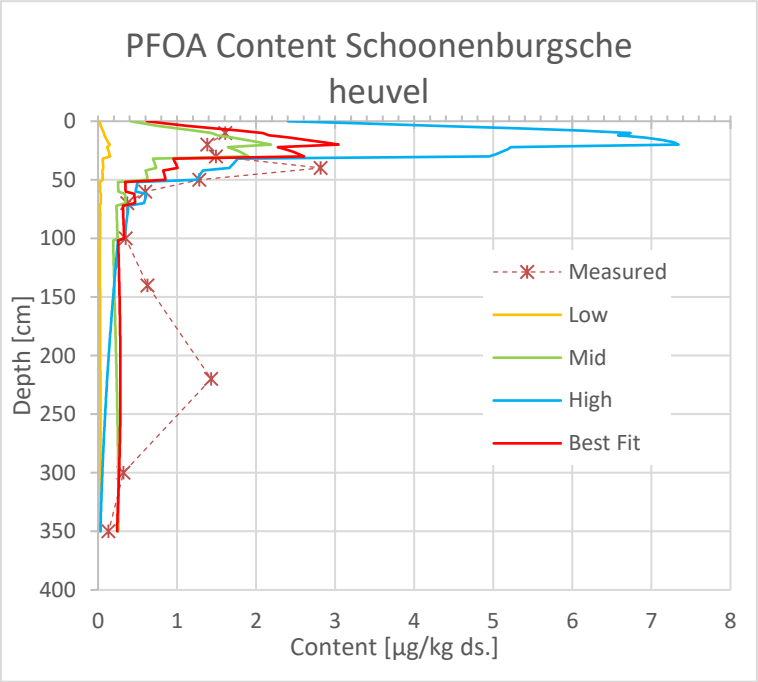

Figure 16. Measured and simulated PFOA content at Schoonenburgsche heuvel.

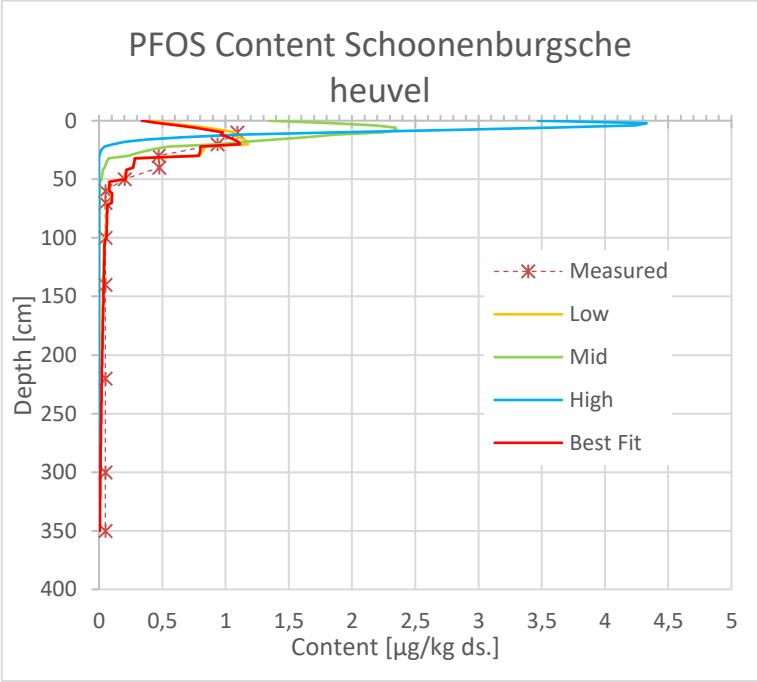

Figure 17. Measured and simulated PFOS content at Schoonenburgsche heuvel.

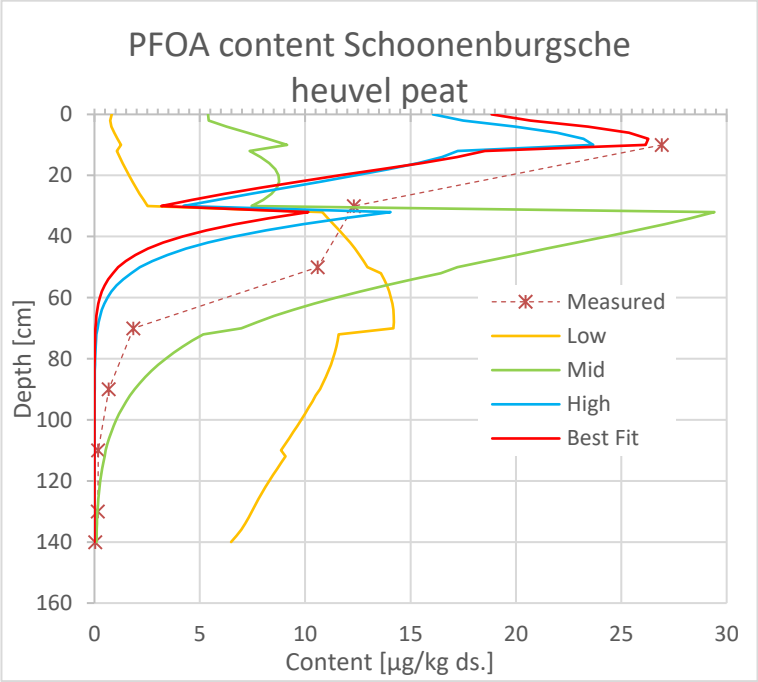

Figure 18. Measured and simulated PFOA content at Schoonenburgsche heuvel peat.

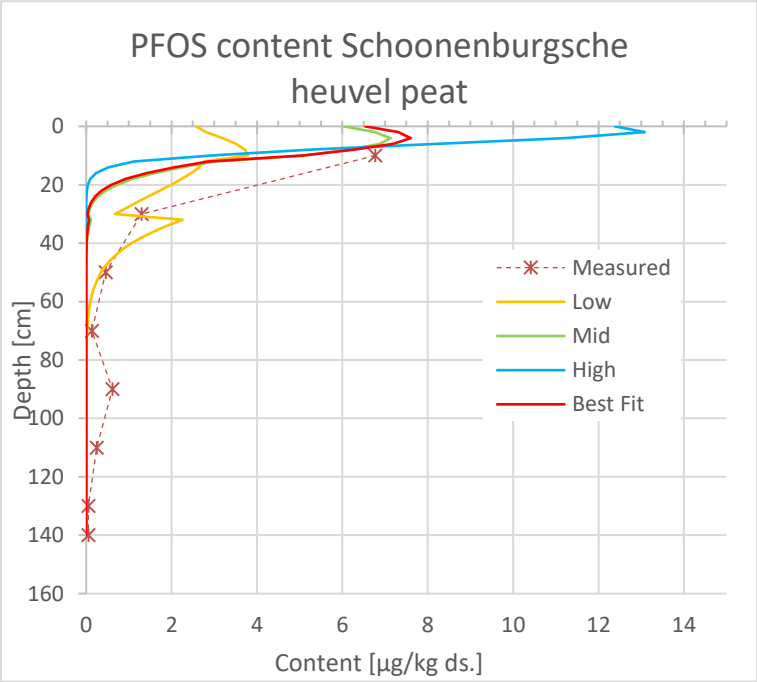

Figure 19. Measured and simulated PFOS content at Schoonenburgsche heuvel peat

Cumulative PFOA/PFOS
Next, the simulated, cumulative PFOA and PFOS contents in the soil profiles are presented. Figure 20 shows the cumulative PFOA as percentage in each soil profile starting from 1970. The best fit simulations were used to prepare this graph that runs from 1970-2070. Atmospheric data of 2012-2020 was extrapolated to 2070 in order to predict the fate of PFAS for the sites studied. The concentration PFOA and PFOS was specified as explained in Chapter 3.4.2.3. It is reminded that the input of PFOA and PFOS started in 1970 and stopped in 2012, when Chemours stopped using PFOA in their factory. The Schoonenburgsche heuvel peat simulation shows that in 2012, 100% of the PFOA was present in the soil profile and remains in the profile during the rest of the simulation. In Hoornaar, the PFOA content reaches 95% because drainage from the bottom already starts before all PFOA had been deposited on the soil surface. The same holds for De Donk and Schoonenburgsche heuvel. It takes about 30-40 years for PFOA to reach the bottom of the 2-3 m deep profiles. In 2070, the PFOA content remaining in the profiles is 20% at Hoornaar and 10% at De Donk and Schoonenburgsche heuvel. This implies that in 2070, the majority of the PFOA has washed out from these sandy soil profiles and has entered the groundwater compartment.

The PFOS graph has a similar trend but more PFOS remains in the profile, see Figure 21. PFOS is released from the bottom of the profiles only after 2012 because all profiles first reach 100% PFOS content, so 100% influx and no outflux. This illustrates that PFOS infiltrates much slower than PFOA.

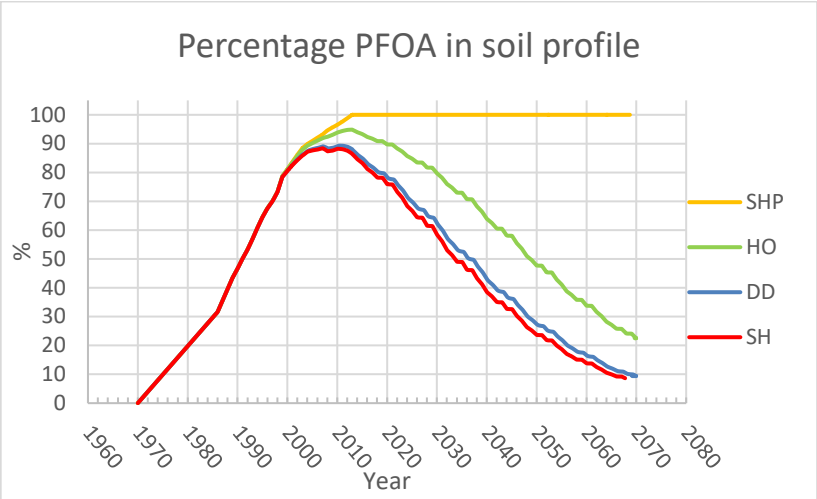

Figure 20. Cumulative PFOA after 100 year simulation.

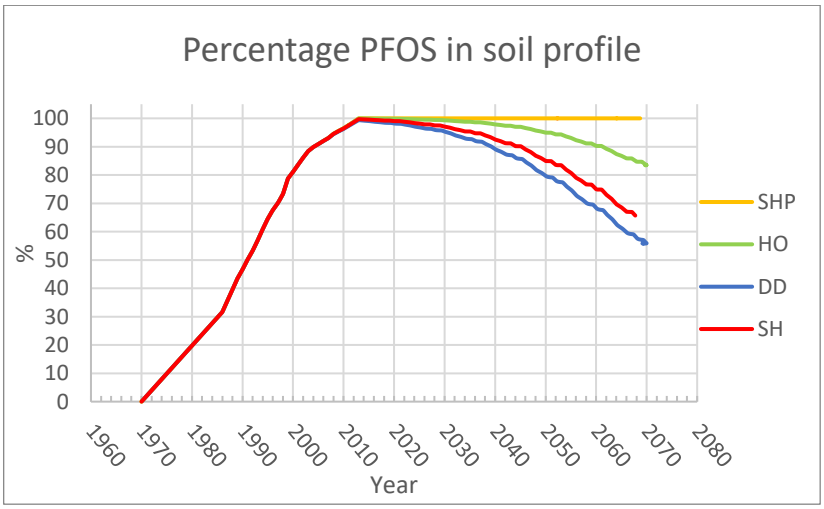

Figure 21. Cumulative PFOS after 100 year simulation.

Sensitivity analysis.
Finally, several model results are presented to show the effect of model choices on the shape of the simulated profiles. A sensitivity analysis was carried out to verify how sensitive the results are to parameter choices. A few parameters had some degrees of freedom when specifying them. The parameters that have the most influence on the shape of the profiles are (1) the K_{oc}, (2) whether f_{oc} is OM based or OC based, (3) the assumed concentration in the precipitation as a function of time (deposition scenario) and (4) discretization of the soil profile in the model (i.e., the number of layers in the soil). The influence of (1) was already presented in Figures 12-19.
The influence of (2) is presented in Figure 22. The ratio of OM to OC varies for every sediment sample (Figure 6). The OC based profile has a somewhat stronger vertical gradient from 20-50 cm. This can directly be related to the OC values in Figure 6.
The influence of (3) is presented in Figure 23. Two profiles are compared: one that takes into account the historical emission from Chemours as far as can be reproduced (explained in Chapter 3.4.2.3) and one that keeps the concentration constant during the emission period. The constant concentration simulation shows that the content in the top 100 cm is higher than with the emission based simulation. From 100-300 cm, the emission based concentration simulation has higher contents than the constant concentration simulation. It was verified how much PFOA was still left in the profile in 2020. Both constant and emission based simulations have very similar bottom flux curves but the top flux curves are different, see Figure 24. The gradient of the top flux of the constant concentration simulation is constant, as it should be. The gradient of the top flux of the emission based concentration simulation changes in time. The gradients represent the PFAS concentration in the precipitation: The steeper the gradient, the higher the concentration (Table 4 shows how the concentrations in time(periods) relate to each other over time).
The influence of (4) is presented in Figure 25. Figure 25 shows that a better fit is obtained when more models layers are used. The peak in the 6 layer simulation is not as sharp as the 5 layer simulation and contents above 1 µg/kg dry soil reach deeper. After these analyses, it was chosen to increase the number of layers, keep the f_{oc} OM based and to keep using an emission based (precipitation) concentration.

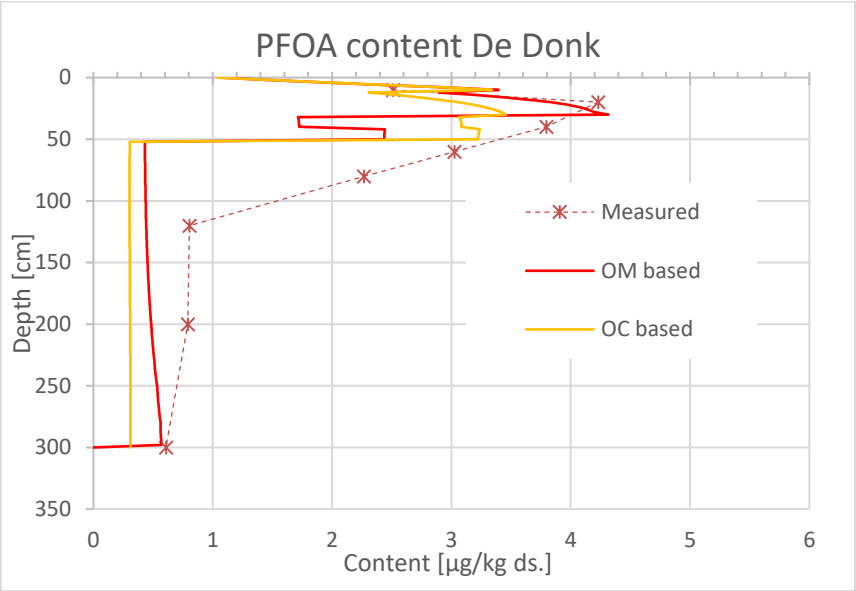

Figure 22. Simulated PFOA content based on OM and OC contents versus measured PFOA content.

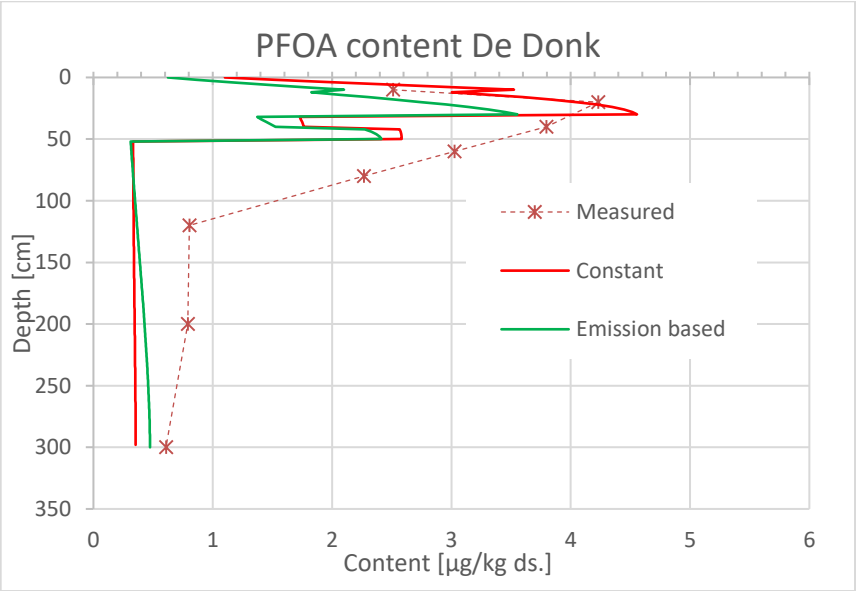

Figure 23. Simulated PFOA content with constant PFAS concentration in precipitation and emission based concentrations, compared to the measured PFOA content.

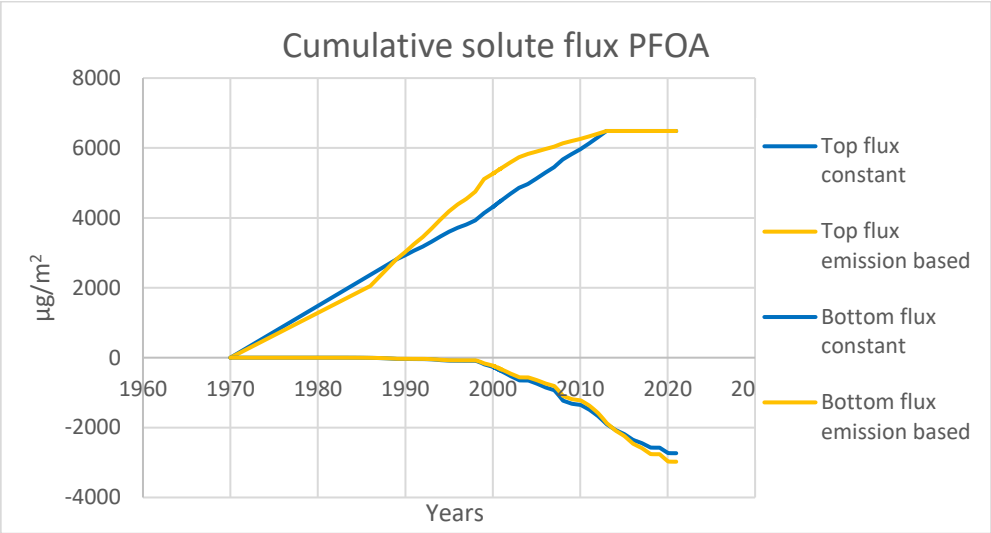

Figure 24. Cumulative surface and bottom solute fluxes a using constant and emission based concentration scenario.

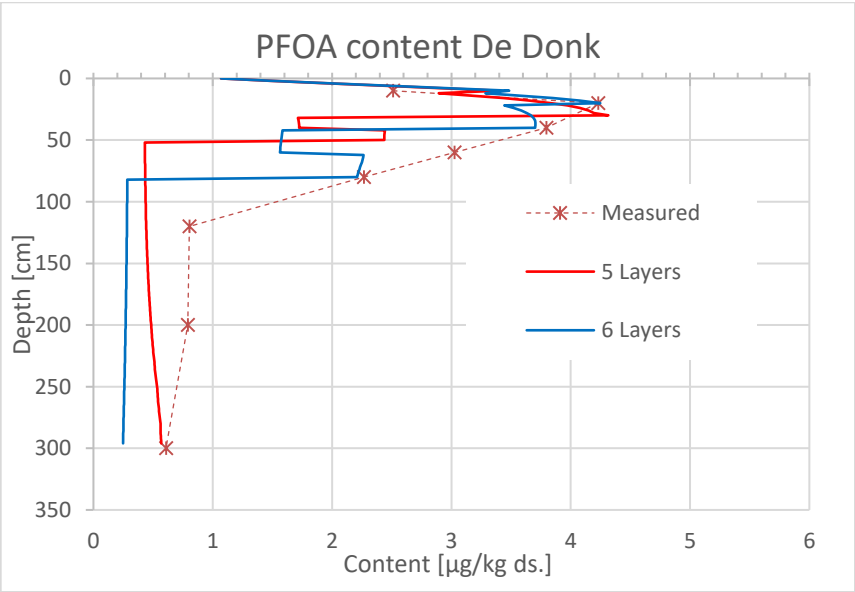

Figure 25. Simulated PFOA content using layer discretization of 5 layers versus 6 layers.

5 Discussion

The research questions form the structure of this chapter in which the results are discussed. First, the results are discussed and their significance is put in broader context. Then the limitations of this study are mentioned Finally, suggestions for follow up research are given.

1. What is the effect of soil properties on the occurrence of PFAS in the unsaturated zone?

The first goal was to explore whether a clear content-depth profile would be found in soils. The LC-MS results in Chapter 4.1.3 show that there is a content-depth profile in the soils with the general trend of decreasing PFOA/PFOS content with increasing depth. The PFOA content is clearly higher than the PFOS content in all measured profiles, consistent with PFOA being the dominant PFAS component in the historical Chemours emissions (Zeilmaker et al., 2016; Pancras et al., 2018). The peat profiles have the highest PFOA & PFOS contents, consistent with their high organic matter content and known interactions between PFOA and PFOS with organic matter (Nguyen et al., 2020). More on the shape of the profiles is discussed under research question two on the next page.

No accumulation of PFOA and PFOS was detected near groundwater level which is in contrast to the statement made in Pancras et al. (2018). They state that PFAS accumulates near air-water interfaces because of the surfactant properties of PFAS. Costanza at al. (2019) state that ”*It is well known that perfluorooctanoic acid (PFOA) and perfluorooctanesulfonic acid (PFOS) accumulate at the air−water interface with a maximum surface excess of ca. 2 mg/m^2 for aqueous concentrations greater than 100 mg/L”.* These concentrations are much higher than the concentrations in the samples from the this research which explains why accumulation near groundwater (air-water interface) did not occur.

The second goal was to investigate whether different soils would show a notably different content-depth profile, assuming a similar atmospheric deposition history. The Schoonenburgsche heuvel and Schoonenburgsche heuvel peat locations are geographically very close to each other so they are compared to discuss whether soil characteristics influence the PFAS content-depth profiles. It was calculated that the total amount of PFAS deposition at Schoonenburgsche heuvel and Schoonenburgsche heuvel peat was very similar (Table 7), confirming the assumption that these soils have been exposed to a similar deposition.

The PFOA content at Schoonenburgsche heuvel peat reaches less deep than in Schoonenburgsche heuvel, has a higher ‘peak’ content and shows slightly different features than the Schoonenburgsche heuvel profile. The peak content of Schoonenburgsche heuvel peat is at ground level. This is most likely related to the much higher organic fraction at Schoonenburgsche heuvel peat (Figure 6), as is consistent with the HYDRUS model simulations. The organic fraction causes higher sorption which increases the potential for PFOA molecules to adsorb to soil particles in the first 20-30 cm of soil. Although there is clay present in SHP-20 and SHP-50 cm, there is no clear indication from the measured profile as well as the model simulations that clay plays an important role with regard to sorption.

The difference in PFOS content-depth profiles between Schoonenburgsche heuvel peat and Schoonenburgsche heuvel is that the peak content of the peat profile is 6 times higher. The shapes of both profiles are very similar.

Li et al. (2018) critically analyzed data of 23 PFOS and 16 PFOA studies. The total data points for studies on PFOS was n = 178. They found a relation of $R^2 = 0.05$ for the relation K_d/OC but the relations were significant ($P < 0.05$). Although Li et al. (2018) concluded that taking only OM into account as a sorption compound is a strong oversimplification of the sorption mechanism of PFAS, the evidence in laboratory and field studies show that OM has a dominant role in sorption behaviour (Milinovic et al., 2015; Higgins & Luthy, 2006). This is in line with the result of this study. Pereira et al. (2020) state that qualitative understanding of interaction of PFAS and iron (hydr)oxides is crucial when the OM faction is low. However, at De Donk, Schoonenburgsche heuvel and Hoornaar there is no indication that sorption mechanisms other than OM have played a significant role.
Peat soils are very different from sand soils, so other mechanisms could have played a role on the sorption behaviour of PFAS. Still, the simulations show that a relatively good description can be achieved using OM alone as sorption mechanism. A point to mention is that when measuring PFAS in soil samples, one collects samples from the field so both the adsorbed *and* dissolved PFAS is measured as PFAS present without distinction. Peat has a much higher porosity than sand and as the groundwater level was 20 cm below ground level the pores in the peat are fully saturated with water. Therefore, the measured adsorbed PFAS might be a slight overestimation. However, the OM and thus K_d is high so most of the PFAS molecules will be adsorbed to OM. It was tested whether this is the case in the model simulations. The highest ratio of suspended (PFOA) to adsorbed (PFOA) was around 1/20, so 5% of the PFOA was suspended.

The PFOA profiles of Schoonenburgsche heuvel, De Donk and Hoornaar share a similar shape, likely because they consist of the same type of sand that stems from the same sedimentological origin. Deeper than 50 cm depth, these soils are very homogenic (Appendix D). Since the soils of Schoonenburgsche heuvel, De Donk and Hoornaar are very comparable in composition, the difference in profile shape is a matter of different deposition history. Taking into account distance to the source and wind direction (Table 7), the results follow a logic line of reasoning: the further away from the source, the lower the cumulative amount of PFAS. It should be noted that wind direction is an important factor, because De Donk is geographically further away from the source than Schoonenburgsche heuvel and Schoonenburgsche heuvel peat but the cumulative amount of PFAS is higher. This is due to the fact that De Donk lies more directly in the common wind direction in relation to Chemours. Another observation from Table 7 is that the closer to the source, the higher the PFOA/PFOS ratio. This strengthens the evidence that PFOA contamination in the soils in this area is linked to the emission of Chemours. More how the PFOA/PFOS profiles relate to Chemours is discussed in the next paragraphs.

2. *Can the deposition profile of PFAS be linked to the historical emission of PFAS by the Chemours factory in Dordrecht?*

The profiles are interpreted in more depth in the next two paragraphs followed by a section on the use of HYDRUS in relation to emission history.

PFOA in relation to Chemours
The measured PFOA content-depth profiles in the sandy soils show firstly an increase in content down to some depth, followed by a decrease (See Figure 8). This applies Schoonenburgsche heuvel, De Donk and Hoornaar. The peak OM/OC in sandy soils is often the highest at ground level and decreases with increasing depth (Figure 6). This indicates that the sorption capacity for PFAS is the highest at ground level. Even though the sorption potential (of PFAS to soil) is the highest near ground level, peak PFOA contents are found at some depth. It is very likely that this peak at some depth is the result of the slow transport of PFOA downward in the profile. The samples were taken in October 2020, 8 years after the phasing out of PFAS at the Chemours factory. PFOA has been transported downward in the soil since that time, reducing the PFOA content at ground level. The fact that peak contents are found at depths of 20-50 cm below ground level is an indication that deposition of PFOA has become less or stopped.
The HYDRYS simulations further support these findings as the model results show generally adequate simulated depth profiles based on known and fitted interaction parameters (K_{oc}) that fall in the literature range (most notably Nguyen et al., 2020). In 8 years, the travel distance of the peak is 20-50 cm. This velocity is consistent with the 100 year simulation (Chapter 4.2.2.). It is therefore fair to say that the combination of measurements and simulations form a strong indication for a direct link between the content-depth profiles of PFOA and the historical emission from the Chemours factory.

A different pattern is observed in the peat soil. The peak content is located close to ground level in the profiles as the OM fraction is much higher compared to the other three locations. The content-depth profile in the peat soil is more ‘compacted’ compared to the other profiles. The PFOA contents at ground level at Schoonenburgsche heuvel, De Donk and Hoornaar are lower than the peak contents at 20-50 cm depth. This trend is not observed in the Schoonenburgsche heuvel peat profile but it might be possible that with a higher sample interval (e.g. every 2 cm instead of 10-20 cm) this trend could be observed.

This finding is also consistent with earlier measuring campaigns (Expertisecentrum PFAS, 2018) that roughly find the same pattern: PFOA content in this region increases in the first 20 cm and then decreases with depth. In comparison to that specific research, the PFOA contents of the samples in this research are rather low except for in the peat samples. This can be explained by the fact that for this research, river dunes were selected as sample locations. These locations have a higher sand fraction and likely less organic matter in the top layer than the surrounding area. Secondly, the sample locations in the mentioned 2018 research are close to roads and buildings. These soils might have been disturbed and the possibility of anthropogenic influence on those soils is more likely than in the soils from this study.

PFOS in relation to Chemours
The measured PFOS profiles are very similar to the measured PFOA profiles but the contents are much lower. The PFOS peak contents are found at shallower depths, closer to the ground level. This is consistent with the model results, based on known and fitted interaction parameters (K_{oc}). The shallower peak content is explained by the fact that PFOS adsorbs stronger to OM, hence the shallow penetration depth of PFOS. Secondly, the Chemours factory did not utilize PFOS (van Bentum et al., 2017) so the deposition history is different from the deposition history of PFOA. PFOS was emitted from another source that is most likely a waste incineration facility which are known for emitting many types of PFAS (Pancras et al., 2018). Typically, the temperature of the incinerator is insufficient to completely break down the PFAS. The ATM incinerator in Moerdijk is geographically the closest incineration facility. In addition to that, ATM is located upwind of the sample locations. Van Bentum et al. (2017) also mention HVC in Dordrecht as potential source.

It is possible that PFOS has a peak at some depth below ground level, just like the PFOA content peaks at De Donk, Hoornaar and Schoonenburgsche heuvel, but that this peak is more shallow (e.g. within the top 10 cm soil) and narrower than the sample interval used in this study. A high sample interval is needed to verify this.

HYDRUS-1D simulations.
The second goal was whether HYDRUS could be used to simulate emission history of the Chemours factory. The results from the HYDRUS simulations show that simulated profiles can be created using soil, solute and water flow parameters. This means that using K_{oc} values from literature, simulation can be made that show characteristics similar to the measure profiles. There is not a very consistent trend found as to which K_{oc} value is best used. This variable is profile specific, and without a measured profile it is not simply possible to say what an actual content/depth profile would look like. However, it is possible to sketch a range of content-depth profiles that often adequately describe the measures profiles. When cumulative deposition and soil/solute/water parameters are known, the model can be used to predict between which extremes the PFOA or PFOS content can be expected.

HYDRUS is a typical example of a mechanistic model: it uses laws of physics to calculate output and can be used in many types of situations and for different purposes. This is valuable in itself, but PFAS interactions and transport in soils is complex and not well understood, which makes it one bridge too far to use HYDRUS for making mechanistic predictions on PFAS transport. Instead, HYDRUS proves be useful in understanding the relation between soil and solute parameters and PFAS transport. The fact that the model simulations show a reasonable match with the measured profiles shows that the transport mechanism is fairly well understood although there is definitely room for improvement. For example, Li et al. (2019) state that there are indications that protein content rather than OM is the dominant property with regard to sorption and that anion exchange capacity is also an important parameter to consider (Li et al., 2019). Other research by Pereira et al. (2018) emphasizes that Fe oxides and soil pH play a role on the interaction between PFAS and OM. Improved understanding leads to better estimates of input parameters which can further decrease the extremes of the range of simulated content-depth profiles.

The to-be released HYDRUS version of Silva et al. (2020) may improve the predictability value of the model. It will likely incorporate new parameters that describe the retardation factors better.

What can be learned from the modelling part of this study is that if one is interested in simulating PFAS transport in soils, one parameter seem to be of key importance which is the K_{oc}. All other parameters definitely have some effect on the shape of the profiles but the K_{oc} is by far the most influential when it comes to profile shape. It is not possible to determine what emission history was like quantitatively (cumulative or in kg/y). In theory, two different emission scenarios with two different K_{oc} values could result in the same content-depth profile. It is therefore not simply possible to quantitatively determine emission history by using inverse modelling of some sort. However, it is possible to describe PFOS/PFOA in the soil in a qualitative sense. The simulations show a range of profiles on which the measured profiles lie. HYDRUS can be very useful in working out what-if scenarios like: ”When will PFAS reach the bottom of a soil layer?” or ”What happens when I extend my profile depth, change texture class or alter the ground water level?”. For instance it was tested how the PFAS content would develop in the next 50 years (Figures 20 & 21). PFOS reaches the bottom of the profile but much later and in lesser contents than PFOA.

Limitations
Limited data was available on emission history from Chemours in the initial period 1970-1990, so the emission based concentration scenario in the period 1970-1990 is subject to large uncertainties. After 1990, there was sufficient data to base the concentration scenarios on. As for the methods in general, the TGA, CS elemental and grain size analysis are routine procedures and were sufficiently accurate for the purpose of this research. The LC-MS analysis was conducted conform standard TNO protocol with the exception of a 9-fold calibration sequence. The internal standard that was used is regarded by TNO as adequate control measure for reliable results although more precision could have possibly been achieved with a calibration sequence.

Recommendations
It would be interesting to see whether there is a relation between PFOS and the waste incineration facility in Moerdijk. A measurement campaign similar to that of Zeilmaker et al. (2016) would be suitable to approach such investigation. Once the version of Silva et al. (2020) is released for public use (this year or in 2022) it would be interesting to repeat the modelling part of this study with the new version to see whether the simulations result in a better fit with the measured profiles. Also, an interesting subject would be to repeat this study and to verify whether PFAS content in soil closer and further away from Chemours is a matter of scaling. For this, the researcher would need to collect samples in the vicinity of the factory (50 km radius) and samples outside the radius with as much as possible similar soil properties. This could be done for e.g. 5 different soils, so 5 ‘paired’ soils. If PFAS content at locations outside the vicinity proves to be a matter of scaling of the contents within the vicinity (assuming similar soil properties) this relation can be used to forecast/predict PFOA content in the region, possibly even including cumulative PFOA amounts. This could be done using the same locations as in Pancras et al. (2018-2).

For the researcher, it is advisable to find out the effect that model parameters have on the outcome of the model early on in the modelling process. Parameters that you think are important or critical in your model might not be the same as the parameters that actually have the largest influence on your model results. For instance, you might think that bulk density of soil has a large effect on PFAS transport but that parameter does not actually change your results much if you alter it. It is recommended to verify these kind of assumptions by testing what effect which parameter has early on.

6 Conclusions

This research aimed to observe the effect of soil properties on the occurrence of PFAS in the unsaturated zone. It was investigated whether there would be a notable difference between the content-depth profiles in different, undisturbed soils with vertical rainwater infiltration that were subjected to similar historical deposition of PFOA and PFOS. The results of the LC-MS analysis show that PFOA and PFOS is detected in most of the samples down to 3 m and 1.2 m depth respectively. The contents detected are at most 27 µg/kg ds. for PFOA and 6.8 µg/kg ds. for PFOS. There is a notable difference between the contents of PFOA and PFOS in sandy soils versus the peat soil. PFOA penetrates deeper in sandy soils and the peak content is located 20-50 cm deeper than in the peat soil. PFOS penetrates deeper in sandy soils than in the peat soil but the peak contents in both soils are located equally deep.

The second aim was to investigate whether the concentration-depth profiles of PFAS could be linked to the historical emissions from the Chemours factory by using HYDRUS-1D to simulate the PFAS transport in soil, based on a reconstructed emission and deposition history of the factory. The measured peak contents of PFOA are found at some depth (20-50 cm) while the highest sorption capacity (highest OM/OC fraction) is near ground level in the sandy soils. This is consistent with the simulated content-depth profiles from HYDRUS, where a similar pattern is observed, based on literature-derived ranges of interaction parameters between PFAS and organic carbon (K_{oc} values). It is very likely that the observation of the peak concentrations at some depth and not at ground level can be attributed to the fact that since 2012, no more deposition of PFOA has taken place. Based on the combination of measurements and modelling results, it is therefore concluded that the content-depth profiles and their shape can be related to the emission (history) of Chemours. PFOS was not emitted by Chemours and its content-depth profile can therefore not be related to their historical emission. It is conceivable that the PFOS in the region of this research originates from the nearest waste incineration facility, ATM Moerdijk.

The model results show that content-depth profiles similar to the measured profiles can be created using independently estimated soil, solute and water flow parameters. The model results provide a range of simulated profiles based on a literature range of the organic carbon-PFAS interaction parameter K_{oc} and historic emission. In general, the simulated content-depth profiles describe the measured content-depth profiles adequately. In addition, HYDRUS proves to be a useful tool to work out ‘what-if’ scenarios and to understand the relations between soil and solute parameters and PFAS transport. Based on the best-fits model scenarios, PFAS contents are projected to decrease in the topsoil as a result of gradual transport to groundwater on a time scale of decades. Finally, HYDRUS is a mechanistic model and PFAS transport is not understood well enough in a mechanistic way. Therefore, more detailed knowledge on interaction of PFAS with soil components is needed to further indicate which soil properties are controlling the sorption intensity in addition to sorption described by a K_{oc} approach.

References

3M. Soil Adsorption/Desorption Study of Potassium Perfluorooctane Sulfonate (PFOS); 3M: St. Paul, MN, 2000, U.S. Environmental Protection Agency Docket AR 226-1030a 030.

Bentum, E van., Pancras, T., Slenders, H., Enden, B van der. (2017). Luchtdepositie onderzoek PFOA en HFPO-DA (GenX) Dordrecht en omgeving. Expertisecentrum PFAS.

Brandsma, S.H., J.C. Koekkoek, M.J.M. van Velzen, J. de Boer, 2019. The PFOA substitute GenX detected in the environment near a fluoropolymer manufacturing plant in the Netherlands. Chemosphere, 220, p. 493-500.

Buck, R. C., Franklin, J., Berger, U., Conder, J. M., Cousins, I. T., De Voogt, P., ... & van Leeuwen, S. P. (2011). Perfluoroalkyl and polyfluoroalkyl substances in the environment: terminology, classification, and origins. Integrated environmental assessment and management, 7(4), 513-541.

Calafat, A. M., Needham, L. L., Kuklenyik, Z., Reidy, J. A., Tully, J. S., Aguilar-Villalobos, M., & Naeher, L. P. (2006). Perfluorinated chemicals in selected residents of the American continent. Chemosphere, 63(3), 490-496.

Carsel, R. F., & Parrish, R. S. (1988). Developing joint probability distributions of soil water retention characteristics. Water resources research, 24(5), 755-769.

Costanza, J., Arshadi, M., Abriola, L. M., & Pennell, K. D. (2019). Accumulation of PFOA and PFOS at the Air–Water Interface. Environmental Science & Technology Letters, 6(8), 487-491.

Costanza-Robinson, M. S., & Henry, E. J. (2017). Surfactant-induced flow compromises determination of air-water interfacial areas by surfactant miscible-displacement. Chemosphere, 171, 275-283.

De Vries, F. (1999). Karakterisering van Nederlandse gronden naar fysisch-chemische kenmerken (No. 654). DLO-Staring Centrum.

DuPont. Adsorption/Desorption of Ammonium Perfluorooctanoate to Soil (OECD 106); E.I. du Pont de Nemours and Company: Wilmington, DE, 2003, U.S. Environmental Protection Agency Docket OPPT-2003-0012-040.

Echa.europa.eu. 2021. Five European States Call For Evidence On Broad PFAS Restriction - All News - ECHA. [online] Available at: <https://echa.europa.eu/nl/-/five-european-states-call-for-evidence-on-broad-pfas-restriction> [Accessed 4 January 2021].

EFSA Panel on Contaminants in the Food Chain (CONTAM), Knutsen, H. K., Alexander, J., Barregard, L., Bignami, M., Brüschweiler, B., ... & Grasl-Kraupp, B. (2018). Risk to human health related to the presence of

perfluorooctane sulfonic acid and perfluorooctanoic acid in food. EFSA journal, 16(12), e05194.

EFSA Panel on Contaminants in the Food Chain (CONTAM), Knutsen, H. K., Alexander, J., Barregård, L., Bignami, M., Brüschweiler, B., ... & Schwerdtle, T. (2018). Risk to human health related to the presence of perfluorooctane sulfonic acid and perfluorooctanoic acid in food. EFSA journal, 16(12), e05194.

EFSA, 2008. Perfluorooctane sulfonate (PFOS), perfluorooctanoic acid (PFOA) and their salts. Scientific opinion of the panel on contaminants in the food chain. 21 february 2008. The EFSA Journal (2008) 653, 1-131.

Favors, M. (2021). Will my exposure to 'forever chemicals' make the Covid-19 vaccine less effective?. Retrieved 10 February 2021, from https://www.theguardian.com/commentisfree/2021/jan/27/will-my-exposure-to-forever-chemicals-make-the-covid-19-vaccine-less-effective

Gibbens, S. (2021). Toxic ‘forever chemicals’ more common in tap water than thought, report says. Retrieved 15 January 2021, from https://www.nationalgeographic.com/science/2020/01/pfas-contamination-safe-drinking-water-study/

Giesy, J. P., Naile, J. E., Khim, J. S., Jones, P. D., Newsted, J. L. (2010). Aquatic Toxicology of Perfluorinated Chemicals. Reviews of Environmental Contamination and Toxicology 202: 1-52.

Hamaker, J. W. and Thompson J. M.: 1972, Adsorption. In Organic Chemicals in the Soil Environment. Vol. 1. (eds C. A. I. Goring and J. W. Hamaker), pp 49. Marcel-Dekker, New York.

Harleman, D., P. Mehlhorn, and R. Rumer (1963), Dispersion-permeability correlation in porous media, J. Hydraul. Div. Am. Soc. Civ. Eng., 89(2), 67–85.

Hazen, A. (1892), Physical Properties of Sands and Gravels With Reference to Their Use Infiltration, Massachusetts State Board of Health, Boston, Mass.

Heiri O, Lotter AF, Lemcke G. 2001. Loss on ignition as a method for estimating organic and carbonate content in sediments: reproducibility and comparability of results. Journal of Paleolimnology 25:101–110.

Helsingør Statement. Scheringer M., X. Trier, I.T. Cousins, P. de Voogt, T. Fletcher, Z. Wang, et al. (2014). Helsingør Statement on poly- and perfluorinated alkyl substances (PFASs). Chemosphere 114:337–339.

Higgins, C. P., & Luthy, R. G. (2006). Sorption of perfluorinated surfactants on sediments. Environmental science & technology, 40(23), 7251-7256.

ISE Report 2001, D. van Dijk, J. Uitenboogaard, P. Pellen en A. Brader. Wageningen Evaluating Programmes for Analytical Laboratories: International Soil-analytical Exchange.

ISE Report quarterly report 99.2 Wageningen Evaluating Programmes for Analytical Laboratories: International Soil-analytical Exchange.
Kasozi GN, Nkedi-Kizza P, Harris WG. 2009. Varied carbon content of organic matter in histosols, spodosols and carbonatic soils. Soil Science Society of America Journal 73:1313–1318

Koch, W.W.R., Droge R., Coenen, P.W.H.G, (2017). Archiefonderzoek historische emissies DuPont Dordrecht. TNO-rapport, TNO 2016 R11743.

Kristensen, S. L., Ramlau-Hansen, C. H., Ernst, E., Olsen, S. F., Bonde, J. P., Vested, A., ... & Toft, G. (2013). Long-term effects of prenatal exposure to perfluoroalkyl substances on female reproduction. Human reproduction, 28(12), 3337-3348.

Laird DA, Chappell MA, Martens DA, Wershaw RL, Thompson M. (2008). Distinguishing black carbon from biogenic humic substances in soil clay fractions. Geoderma 143:115–122

Li, F., Fang, X., Zhou, Z., Liao, X., Zou, J., Yuan, B., & Sun, W. (2019). Adsorption of perfluorinated acids onto soils: Kinetics, isotherms, and influences of soil properties. Science of the total environment, 649, 504-514.

Lijzen, J.P.A., M.P.M. Janssen, R. van Herwijnen, A. Wintersen, M.C. Zijp, L. Posthuma (2011). Verkenning doelstelling voor herstel verontreiniging met PFOS. RIVM Briefrapport 607083001/2011.

Lindstrom A.B., M.J. Strynar, E.L. Libelo (2011). Polyfluorinated compounds: past present and future, Environ. Sci. Technol. 45(19) 7954-7961.

Madrid Statement. Blum, A., S.A. Balan, M. Scheringer, X. Trier, G. Goldenman, I.T. Cousins, M. Diamond, T. Fletcher, C. Higgins, A.E. Lindeman, G. Peaslee, P. de Voogt, Z. Wang, R. Weber (2015). The Madrid statement on poly- and perfluoroalkyl substances (PFASs). Environmental Health Perspectives, Mei 2015, 123:5, A107-A111.

Mastrantonio, M., E. Bai, R. Uccelli, V. Cordiano, A. Screpanti, P. Crosignani (2017). Drinking water contamination from perfluoroalkyl substances (PFAS): an ecological mortality study in the Veneto Region, Italy. Eur J Public Health, May 23.

McDonald’s announces global ban of toxic PFAS chemicals in food packaging by 2025. (2021). YubaNet. Retrieved 15 January 2021, from https://yubanet.com/enviro/mcdonalds-announces-global-ban-of-toxic-pfas-chemicals-in-food-packaging-by-2025/

Milinovic, J., Lacorte, S., Vidal, M., & Rigol, A. (2015). Sorption behaviour of perfluoroalkyl substances in soils. Science of the Total Environment, 511, 63-71.

Moermond, C.T.A., E.M.J. Verbruggen, C.E. Smit (2010). Environmental risk limits for PFOS. A proposal for water quality standards in accordance with the Water Framework Directive. RIVM report 601714013/2010.

Nguyen, T. M. H., Bräunig, J., Thompson, K., Thompson, J., Kabiri, S., Navarro, D. A., ... & Mueller, J. F. (2020). Influences of Chemical Properties, Soil Properties, and Solution pH on Soil–Water Partitioning Coefficients of Per-and Polyfluoroalkyl Substances (PFASs). Environmental Science & Technology, 54(24), 15883-15892.

Nieuwe achtergrondwaarden voor twee soorten PFAS. (2021). Retrieved 4 January 2021, from https://www.rivm.nl/nieuws/nieuwe-achtergrondwaarden-voor-twee-soorten-pfas#:~:text=Voor%20PFOS%20adviseert%20het%20RIVM,microgram%20per%20kilogram%20droge%20stof.&text=PFAS%20zijn%20door%20de%20mens,niet%20in%20het%20milieu%20voorkomen.

Noorlander, C.W., J.D. te Biesebeek, S.P.J. van Leeuwen, M.J. Zeilmaker (2010). Intake of PFOS and PFOA from food and drinking water in the Netherlands. RIVM Letter report 320126001/2010.

Olsen, G.W. J.M. Burris, D.J. Ehresman, J.W. Froehlich, A.M. Seacat, J.L. Butenhoff, L.R. Zobel (2007). Half-life of serum elimination of perfluorooctanesulfonate, perfluorohexanesulfonate, and perfluorooctanoate in retired fluorochemical production workers. Environmental Health Perspectives, September 2007, 115:9, 1298-1305.

Pallasser, R., Minasny, B., & McBratney, A. B. (2013). Soil carbon determination by thermogravimetrics. PeerJ, 1, e6.

Pancras, T., Bentum, van E., Slenders, H. (2018). Poly- en PerFluor Alkyl Stoffen (PFAS). Expertisecentrum PFAS. DDT219-1/18-009.764

Pancras, T., Bentum, van E., Slenders, H. (2018-2). Aanwezigheid van PFAS in Nederland. Expertisecentrum PFAS. DDT219-1/18-008.228

Pancras, T., G. Schrauwen, T. Held, K. Baker, I. Ross, H. Slenders (2016). Evironmental fate and effects of poly and perfluoroalkyl substances (PFAS). Concawe report 8/16.

Paul, A.G., K.C. Jones, A.J. Sweetman (2009). A first global production, emission and environmental inventory for perfluorooctane sulfonate. Environmental Science and Technology, 43: 386-392.

Pereira, H. C., Ullberg, M., Kleja, D. B., Gustafsson, J. P., & Ahrens, L. (2018). Sorption of perfluoroalkyl substances (PFASs) to an organic soil horizon–Effect of cation composition and pH. Chemosphere, 207, 183-191.

Pérez, F., Llorca, M., Köck-Schulmeyer, M., Škrbić, B., Oliveira, L. S., da Boit Martinello, K., ... & Barceló, D. (2014). Assessment of perfluoroalkyl substances in food items at global scale. Environmental research, 135, 181-189.

Poll, R. van, E. Jansen, R. Janssen (2017). PFOA-metingen in bloed. Metingen in serum bij omwonenden van DuPont/Chemours te Dordrecht. RIVM Rapport 2017-0077.

Prevedouros K, Cousins IT, Buck, RC, Korzeniowski SH (2006): Sources, fate and transport of Perfluorocarboxylates – A critical review. Environ Sci Technol 40, 32–44

Qi, Y., Hu, S., Huo, S., Xi, B., Zhang, J., & Wang, X. (2015). Spatial distribution and historical deposition behaviors of perfluoroalkyl substances (PFASs) in sediments of Lake Chaohu, a shallow eutrophic lake in Eastern China. Ecological Indicators, 57, 1-10.

Review Of Available Software For PFAS Modeling Within The Vadose Zone. 2020. 1st ed. [ebook] Michigan: AECOM, p.9. Available at: <https://www.michigan.gov/documents/pfasresponse/Review_of_Available_Software_for_PFAS_Modeling_Within_the_Vadose_Zone_699324_7.pdf> [Accessed 20 October 2020].

Rigét, F., R. Bossi, C. Sonne, K. Vorkamp, R. Dietz (2013). Trends of perfluorochemicals in Greenland ringed seals and polar bears: Indications of shifts to decreasing trends. Chemosphere 93: 1607-1614.

Rijksinstituut voor Volksgezondheid en Milieu Ministerie van Volksgezondheid, Welzijn en Sport. 2020. Verbod Gebruik PFAS. Available at: <https://www.rivm.nl/pfas/verbod-gebruik-pfas> [Accessed 15 October 2020].

Rosen, M. J., Kunjappu, J. T. Surfactants and Interfacial Phenomena, 4th ed.; John Wiley & Sons, Inc.: 2012.

Schaap, M. G., Leij, F. J., and van Genuchten, M. Th., Rosetta: a computer program for estimating soil hydraulic parameters with hierarchical pedotransfer functions, Journal of Hydrology, 251,

Silva, J. A. K., Šimůnek, J., & McCray, J. E. (2020). A Modified HYDRUS Model for Simulating PFAS Transport in the Vadose Zone. Water, 12(10), 2758.

Silva, J. A., Martin, W. A., Johnson, J. L., & McCray, J. E. (2019). Evaluating air-water and NAPL-water interfacial adsorption and retention of Perfluorocarboxylic acids within the Vadose zone. Journal of contaminant hydrology, 223, 103472.

Šimůnek, J., M. Šejna, H. Saito, M. Sakai, and M. Th. van Genuchten, The HYDRUS-1D Software Package for Simulating the Movement of Water, Heat, and Multiple Solutes in Variably Saturated Media, Version 4.08, HYDRUS Software Series 3, Department of Environmental Sciences, University of California Riverside, Riverside, California, USA, pp. 330, 2008.

Thunnissen, H.A.M. (1987). Eenvoudige methode voor de schatting van verb1ijftijden van grondwater in de verzadigde zone. RIVM, Bilthoven. Rapport nr. 728472002.

Tweede Kamer (2017). Tweede Kamer der Staten Generaal, 28089, 28663, nr. 47. Brief van de staatssecretaris van infrastructuur en milieu aan de voorzitter van de tweede kamer der staten generaal, d.d. 22 juni 2017. Bijlage 1.

van Genuchten, M. Th., A closed-form equation for predicting the hydraulic conductivity of unsaturated soils, Soil Sci. Soc. Am. J., 44, 892-898, 1980.

Weber, A. K., Barber, L. B., LeBlanc, D. R., Sunderland, E. M., & Vecitis, C. D. (2017). Geochemical and hydrologic factors controlling subsurface transport of poly-and perfluoroalkyl substances, Cape Cod, Massachusetts. Environmental science & technology, 51(8), 4269-4279.

Wintersen, A., Spijker, J., van Breemen, P., & van Wijnen, H. (2020). Achtergrondwaarden perfluoralkylstoffen (PFAS) in de Nederlandse landbodem.

Wintersen, A.M., J.P.A. Lijzen, R. van Herwijnen (2016). Milieukwaliteitswaarden voor PFOS: Uitwerking van generieke en gebiedsspecifieke waarden voor het gebied rond Schiphol. RIVM Briefrapport 2016-0001.

Zareitalabad, P., Siemens, J., Hamer, M., & Amelung, W. (2013). Perfluorooctanoic acid (PFOA) and perfluorooctanesulfonic acid (PFOS) in surface waters, sediments, soils and wastewater–A review on concentrations and distribution coefficients. Chemosphere, 91(6), 725-732.

Zeilmaker, M.J., P. Janssen, A. Versteegh, A. Van Pul, W. De Vires, B. Bokkers, S. Wuijts, A. Oomen, J. Herremans (2016). Risicoschatting emissie PFOA voor omwonenden. Locatie: DuPont/Chemours, Dordrecht, Nederland. RIVM Briefrapport 2016-0049.

Appendices

Appendix A. Fieldwork and Laboratory Materials.

Fieldwork materials

- Edelman drill for sand with 5 extension rods and 5 connecting pieces.
- Wide gouge of 2 inches.
- 100 sample jars (250 ml volume).
- 100 sample jars PFAS free (50ml volume).
- 200 labels for the jars.
- 5 x apple corer for taking samples from Edelman.
- Cardboard boxes as outlay sheet for soil samples.
- Tape measure (5m).
- Set of (old) tea towels for cleaning.
- Roll of tissue paper/kitchen paper.
- Knife for cutting and cleaning gouge.
- Bottle of methanol (1.5l) for thorough cleaning of sample equipment.
- GPS
- Sand ruler.
- Plastic bag for waste
- Pens/markers
- Camera
- Plastic boxes for carrying equipment.
- Water level gauge.
- Jerrycan demi water (10l).

Laboratory materials

- Plastic (PP or PE) bottle of 100ml
- 12ml plastic centrifuge tube with screw cap
- Plastic 1.8ml vials with screw cap
- Plastic 0.3ml insert vials with screw cap
- Methanol (Fluka, LC-MS grade)
- Acetonitrile (JT Baker HPLC grade)
- MilliQ water (Millipore system)
- Ammonium format (10M; Fluka AG)
- Ammonia (NH4OH) solution in water (28%; Sigma-Aldrich)
- Formic acid (98%; Fluka AG)- Plastic disposable pipettes.
- Plastic SPE columns 3cc
    - JT Baker, Oasis WAX; 60 mg; 60□
    - Phenomenex, Strata-XL-AW; 60mg; 100□
- Eppendorf Multipette with accompanying combi tips
- Centrifuge, suitable for 12 ml centrifuge tubes and minimum attainable speed of 5000 rpm (Hermle Z 383K)
- Agilent LC-MS system
- LC column: Alltech Alltima HP C18 (250 * 2.1mm; 5□)
- Analytical balance (4 decimal places)

Appendix B. Results TGA.

	Thermogravimetric analysis							
Name	Weight Initial [g]	Weight Dry [g] = 100%	Weight dry [%]	Weight loss 105-450°C [%] OM-range	Weight loss 450-550°C [%]	Weight loss 550-700°C [%]	Weight loss 700-850 °C [%]	Weight loss 850-1000 °C [%]
DD-10	4.560	3.663	80.30	6.13	0.30	0.18	0.07	0.11
DD-20	4.632	3.860	83.34	5.20	0.30	0.17	0.06	0.11
DD-40	4.526	3.712	82.02	4.08	0.26	0.26	0.05	0.05
DD-60	4.668	4.184	89.65	1.75	0.17	0.27	0.06	0.03
DD-80	4.803	4.211	87.67	2.54	0.19	0.37	0.06	0.03
DD-120	4.700	4.603	97.94	0.37	0.09	0.10	0.06	0.03
DD-200	4.411	4.260	96.58	0.29	0.10	0.10	0.06	0.03
DD-300	4.767	4.601	96.52	0.32	0.09	0.09	0.05	0.03
HO-5	4.739	3.938	83.10	4.88	0.27	0.13	0.06	0.07
HO-10	4.895	4.323	88.32	3.16	0.24	0.14	0.08	0.06
HO-20	4.778	4.218	88.27	2.90	0.23	0.13	0.08	0.04
HO-30	4.617	4.094	88.67	2.48	0.20	0.13	0.07	0.04
HO-40	4.864	4.363	89.69	1.72	0.16	0.12	0.07	0.04
HO-50	4.372	3.997	86.25	3.43	0.31	0.16	0.09	0.05
HO-60	4.390	3.771	91.05	1.28	0.13	0.10	0.05	0.04
HO-70	4.857	4.494	92.53	1.02	0.10	0.08	0.09	0.07
HO-100	4.639	4.468	96.32	0.32	0.08	0.08	0.09	0.07
HO-150	4.340	4.232	97.51	0.30	0.09	0.09	0.05	0.03
HO-200	4.480	4.147	92.56	0.29	0.08	0.08	0.04	0.03

HO-250	4.889	3.833	78.41	0.25	0.08	0.08	0.05	0.03
SH-10	4.691	3.832	81.70	6.08	0.30	0.15	0.07	0.10
SH-20	4.543	3.729	82.10	5.53	0.28	0.20	0.07	0.07
SH-30	4.885	4.282	87.65	3.94	0.23	0.13	0.08	0.06
SH-40	4.863	4.652	95.67	1.42	0.15	0.13	0.06	0.04
SH-50	4.447	4.172	93.82	1.15	0.15	0.12	0.07	0.04
SH-60	4.871	4.644	95.33	0.46	0.12	0.11	0.06	0.03
SH-70	4.944	4.727	95.61	0.60	0.11	0.11	0.06	0.04
SH-100	4.626	4.497	97.22	0.40	0.12	0.14	0.07	0.04
SH-140	4.971	4.822	97.00	0.35	0.11	0.11	0.06	0.04
SH-220	4.840	4.661	96.30	0.32	0.11	0.11	0.06	0.03
SH-300	4.839	4.584	94.73	0.28	0.11	0.11	0.06	0.03
SH-350	4.861	3.826	78.70	0.28	0.11	0.12	0.07	0.04
SHP-10	4.399	2.466	56.06	23.84	1.50	0.54	0.17	0.42
SHP-30	4.194	2.395	57.11	17.61	1.45	0.44	0.23	0.38
SHP-50	4.058	0.841	20.72	72.87	4.02	1.18	0.08	0.59
SHP-70	4.269	0.528	12.37	75.50	3.18	0.69	0.09	1.15
SHP-90	4.144	0.709	17.10	61.80	4.16	1.17	0.15	1.99
SHP-110	4.379	0.686	15.67	61.50	3.53	0.71	0.28	2.93
SHP-130	4.281	0.652	15.24	63.98	5.03	1.58	0.13	1.89
SHP-140	4.115	0.638	15.50	64.84	4.56	1.28	0.14	1.45

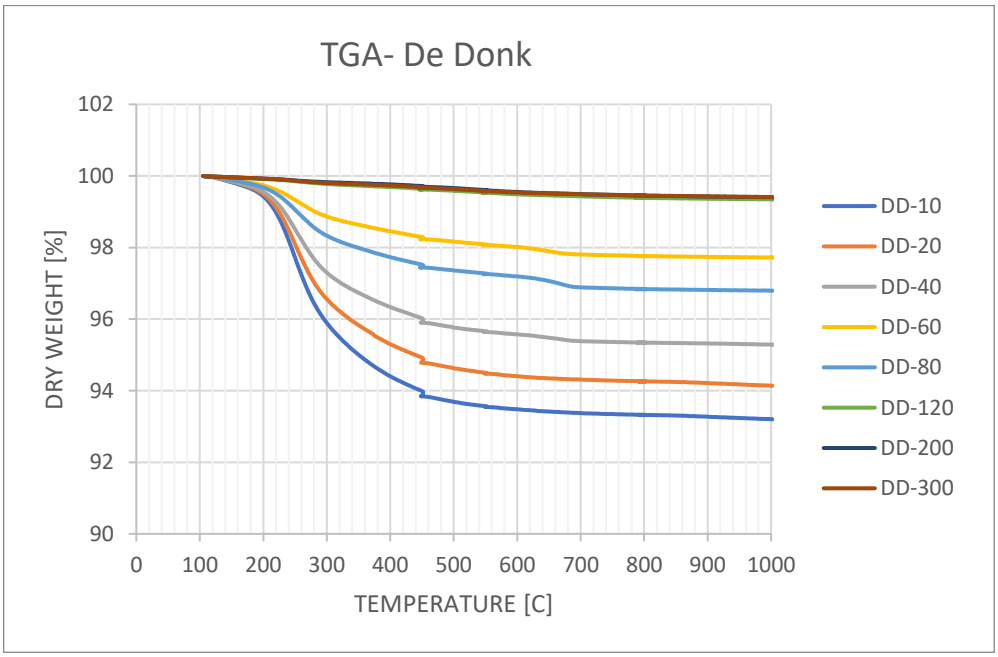
TGA- De Donk
DRY WEIGHT [%]
102
100
98
96
94
92
90
0
100
200
300
400
500
600
700
800
900
1000
TEMPERATURE [C]
DD-10
DD-20
DD-40
DD-60
DD-80
DD-120
DD-200
DD-300

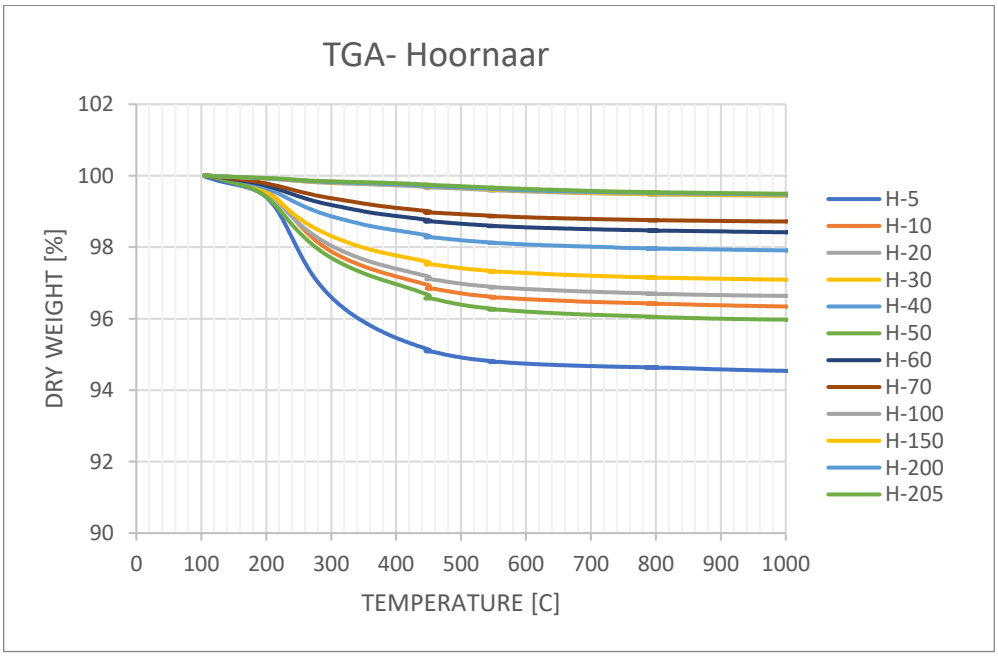
TGA- Hoornaar
DRY WEIGHT [%]
102
100
98
96
94
92
90
0
100
200
300
400
500
600
700
800
900
1000
TEMPERATURE [C]
H-5
H-10
H-20
H-30
H-40
H-50
H-60
H-70
H-100
H-150
H-200
H-205

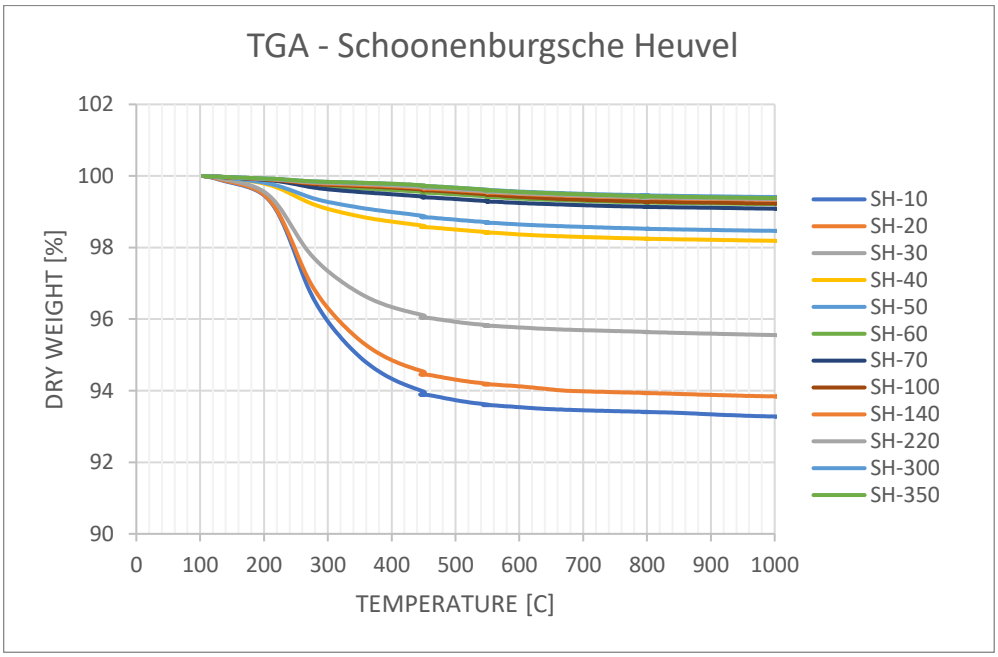
TGA - Schoonenburgsche Heuvel
DRY WEIGHT [%]
102
100
98
96
94
92
90
0
100
200
300
400
500
600
700
800
900
1000
TEMPERATURE [C]
SH-10
SH-20
SH-30
SH-40
SH-50
SH-60
SH-70
SH-100
SH-140
SH-220
SH-300
SH-350

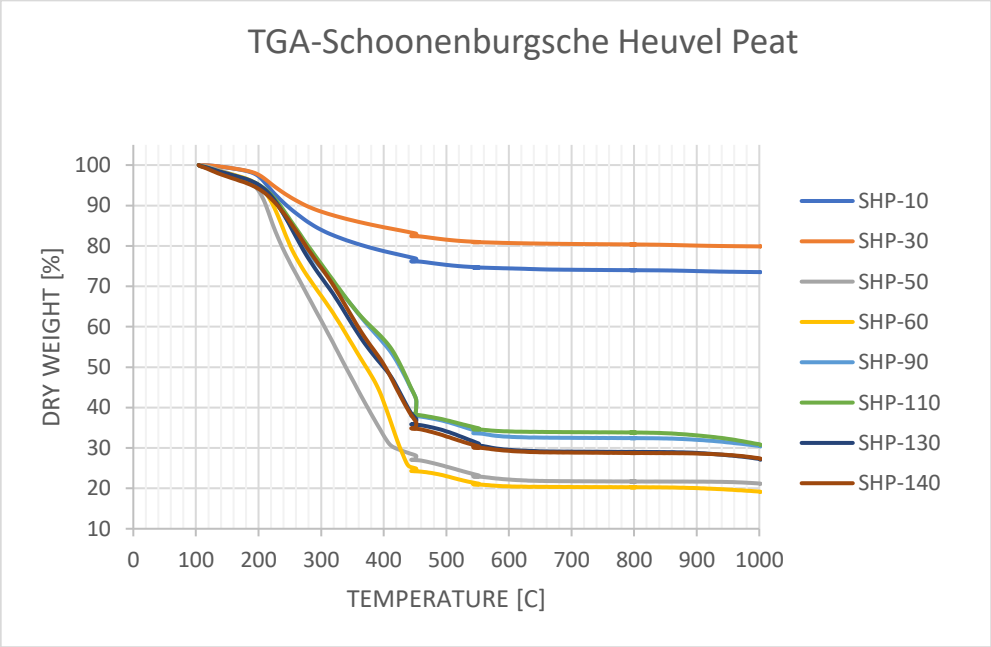
TGA-Schoonenburgsche Heuvel Peat
DRY WEIGHT [%]
100
90
80
70
60
50
40
30
20
10
0
100
200
300
400
500
600
700
800
900
1000
TEMPERATURE [C]
SHP-10
SHP-30
SHP-50
SHP-60
SHP-90
SHP-110
SHP-130
SHP-140

Appendix C. Grain size distribution. CS elemental. Soil moisture and LC-MS.

Sample	Grain Size Distribution				CS	Soil Moisture	LC-MS
Name	D10 [µm]	D50 [µm]	K_s [cm/d]	Corresponding texture class*	OC [% of mass]	θ [0-100]	Content in [µg/kg dry soil]
DD-10	41	287	105	Medium sand	3.82	19.7	2.51
DD-20	46	303	130	Medium sand	2.70	17.6	4.23
DD-40	29	293	52	Medium sand	2.04	17.5	3.79
DD-60	43	321	113	Medium sand	2.09	10.8	3.03
DD-80	25	303	39	Medium sand	2.19	11.4	2.27
DD-120	213	348	2831	Medium sand	0.23	2.1	0.81
DD-200	203	355	2564	Medium sand	0.16	3.2	0.79
DD-300	203	348	2577	Medium sand	0.23	3.6	0.61
H-5	-	-	41	Medium sand	2.41	15.4	0.45
H-10	26	336	46	Medium sand	1.46	11.1	0.57
H-20	27	326	75	Medium sand	1.26	11.6	1.04
H-30	35	333	121	Medium sand	1.26	13.0	1.28
H-40	44	345	69	Medium sand	1.02	11.0	2.43
H-50	33	346	2022	Medium sand	1.39	10.3	2.15
H-60	180	378	2901	Medium sand	1.14	9.4	1.57
H-70	216	379	3259	Medium sand	0.80	0.3	1.41
H-100	229	377	3561	Medium sand	0.20	1.6	0.52
H-150	239	424	3245	Medium sand	0.21	2.6	0.44
H-200	228	372	3403	Medium sand	0.16	7.6	0.19
H-250	234	386	41	Medium sand	0.13	21.2	0.13

SH-10	44	276	121	Medium sand	3.31	18.3	1.61
SH-20	53	284	176	Medium sand	2.88	18.0	1.38
SH-30	48	280	145	Medium sand	1.76	12.4	1.49
SH-40	163	308	1652	Medium sand	1.57	4.5	2.82
SH-50	162	311	1626	Medium sand	1.09	5.5	1.28
SH-60	193	337	2326	Medium sand	0.39	4.4	0.60
SH-70	190	326	2257	Medium sand	0.39	4.6	0.37
SH-100	204	333	2601	Medium sand	0.22	2.6	0.35
SH-140	191	328	2279	Medium sand	0.24	3.1	0.63
SH-220	196	340	2381	Medium sand	0.18	3.9	1.43
SH-300	196	351	2390	Medium sand	0.21	5.3	0.32
SH-350	209	364	2709	Medium sand	0.18	22.1	0.13
SHP-10	4	37	1	Silt	12.21	44.2	26.92
SHP-30	3	19	1	Silt	9.16	43.7	12.31
SHP-50	8	64	4	Very fine sand	49.06	79.8	10.59
SHP-70	-	-	-	Peat	45.65	87.2	1.85
SHP-90	-	-	-	Peat	14.98	86.4	0.69
SHP-110	-	-	-	Peat	35.57	85.9	0.19
SHP-130	-	-	-	Peat	38.55	85.0	0.16
SHP-140	-	-	-	Peat	39.61	85.1	0.05

* Based on USDA classification of soil particle size.

Appendix D. Grain size distribution graphic.

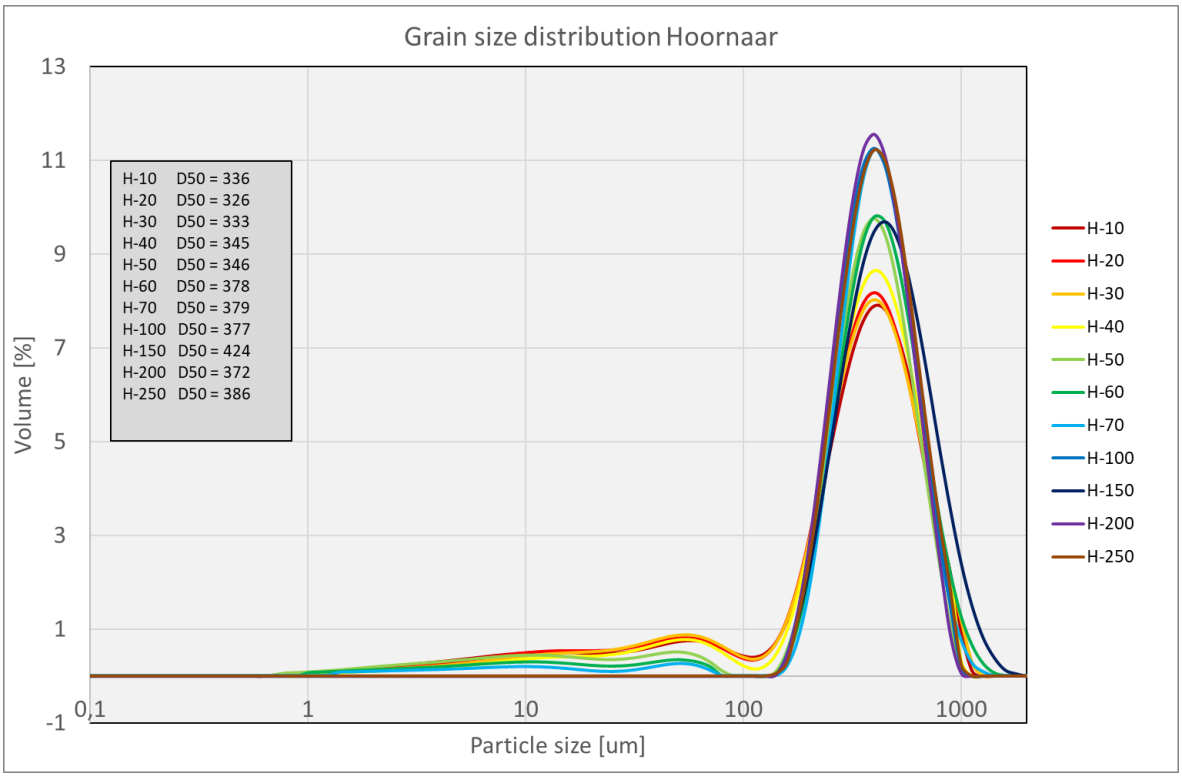

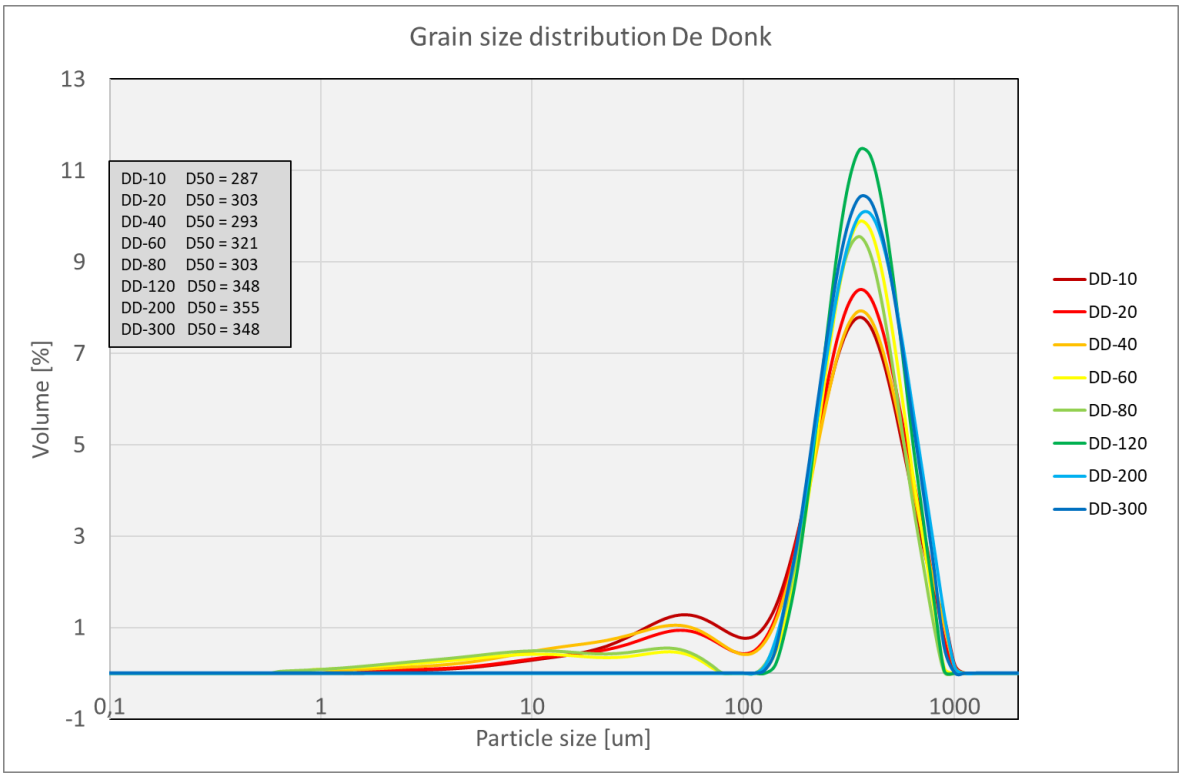

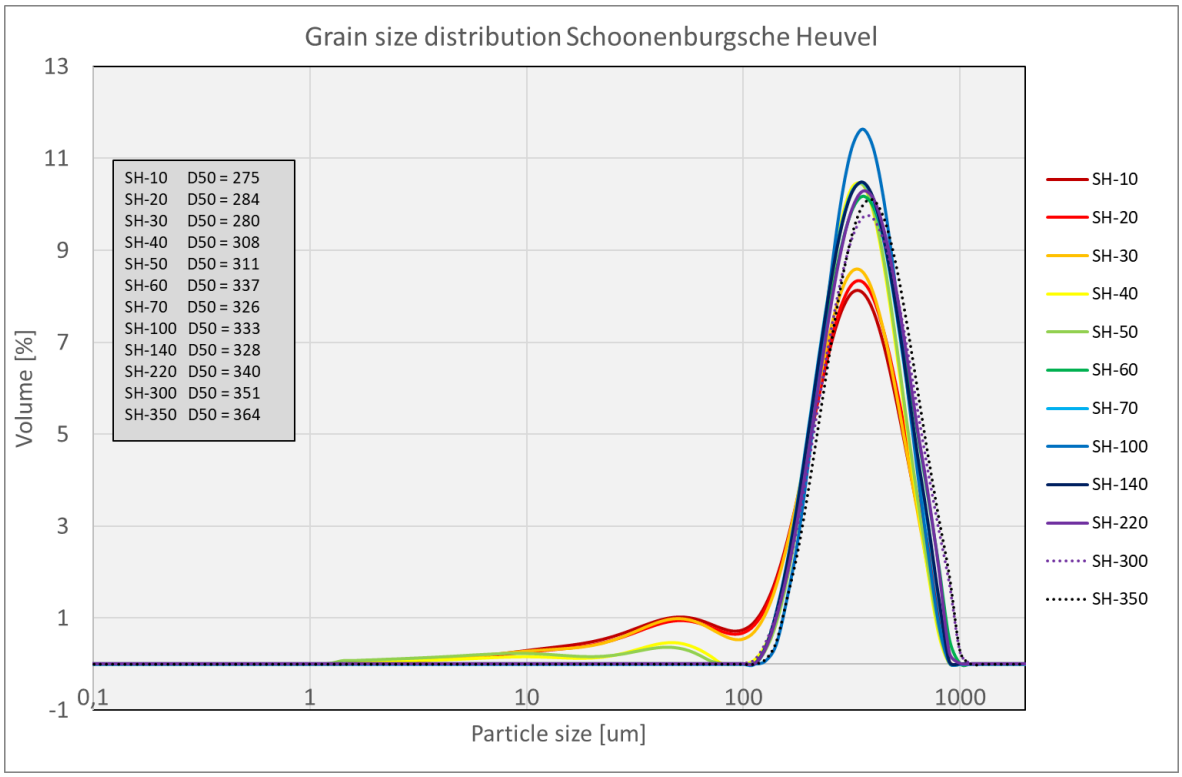
Grain size distribution Schoonenburgsche Heuvel
SH-10 D50 = 275
SH-20 D50 = 284
SH-30 D50 = 280
SH-40 D50 = 308
SH-50 D50 = 311
SH-60 D50 = 337
SH-70 D50 = 326
SH-100 D50 = 333
SH-140 D50 = 328
SH-220 D50 = 340
SH-300 D50 = 351
SH-350 D50 = 364
Volume [%]
Particle size [um]
13
11
9
7
5
3
1
-1
0,1
1
10
100
1000
SH-10
SH-20
SH-30
SH-40
SH-50
SH-60
SH-70
SH-100
SH-140
SH-220
SH-300
SH-350

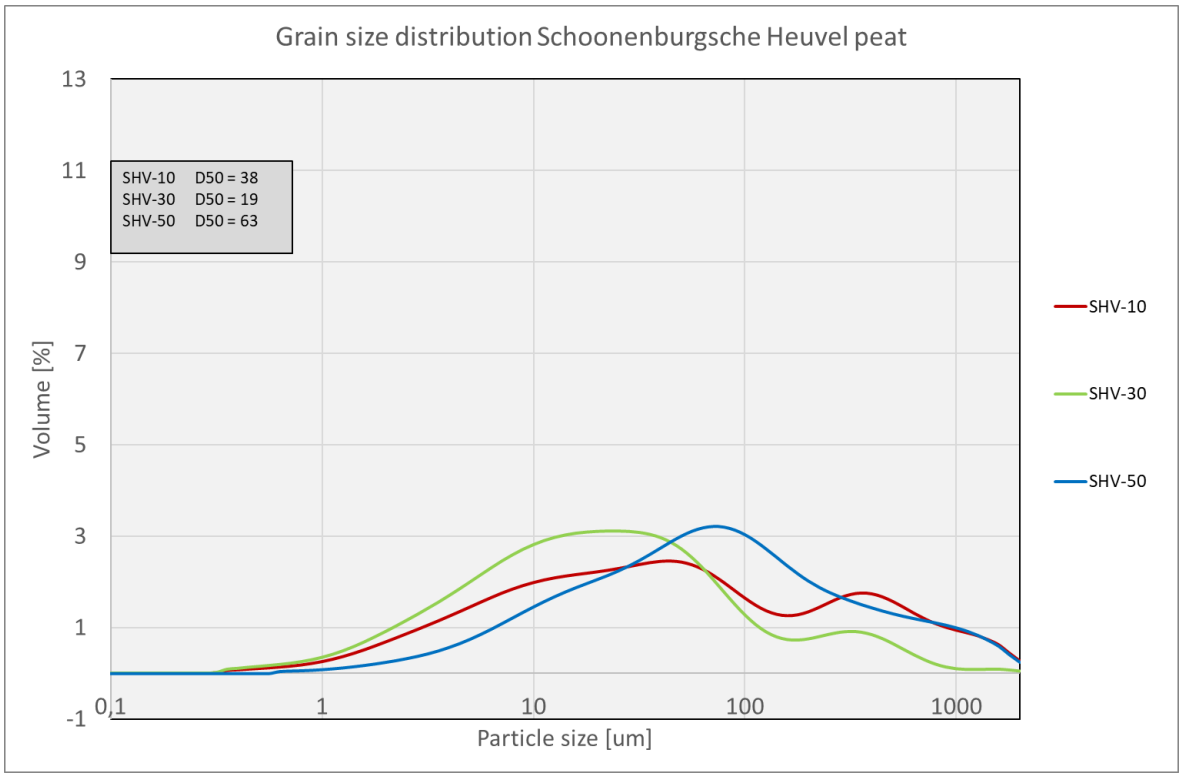
Grain size distribution Schoonenburgsche Heuvel peat
SHV-10 D50 = 38
SHV-30 D50 = 19
SHV-50 D50 = 63
Volume [%]
Particle size [um]
13
11
9
7
5
3
1
-1
0,1
1
10
100
1000
SHV-10
SHV-30
SHV-50

Appendix E. Input parameters HYDRUS.

lay nr	Optie 1 PFOS + Lay	Optie 2 PFOS + Lay	Optie 1 PFOS + Lay	Optie 1 PFOA + Laagjes	Optie 2 PFOA + Laagjes	Optie 3 PFOA + Laagjes	PFOA best fit	PFOS best fit	Bulk density [g/cm3]	Dispersion [cm]	Molecular Diffusion [cm2/d]	Residual soil water content [-]	Saturated soil water content [-]	Parameter ***a*** in the soil water retention	Parameter ***n*** in the soil water retention function [-]	Saturated Ks [cm/year]	Saturated Ks [cm/day]	Tortuosity parameter [-]
1	18,9	47,5	119,4	2,4	7,5	18,9	8,3	13,5	1,5	5	0,47	0,045	0,43	0,145	2,68	127750	350	0,5
2	16,0	40,3	101,2	2,0	6,4	16,0	7,0	11,5	1,5	5	0,47	0,045	0,43	0,145	2,68	127750	350	0,5
3	12,6	31,6	79,4	1,6	5,0	12,6	5,5	9,0	1,5	5	0,47	0,119	0,35	0,014	2	127750	350	0,5
4	5,4	13,6	34,1	0,7	2,1	5,4	2,4	3,9	1,5	5	0,47	0,119	0,35	0,014	2	127750	350	0,5
5	7,8	19,7	49,5	1,0	3,1	7,8	3,4	5,6	1,5	5	0,47	0,119	0,35	0,014	2	255500	700	0,5
6	1,0	2,5	6,4	0,1	0,4	1,0	0,4	0,7	1,5	5	0,47	0,119	0,35	0,014	2	255500	700	1,5

1. Input parameters De Donk.

lay nr	Optie 1 PFOS + Lay	Optie 2 PFOS + Lay	Optie 1 PFOS + Lay	Optie 1 PFOA + Laagjes	Optie 2 PFOA + Laagjes	Optie 3 PFOA + Laagjes	PFOA best fit	PFOS best fit	Bulk density [g/cm3]	Dispersion [cm]	Molecular Diffusion [cm2/d]	Residual soil water content [-]	Saturated soil water content [-]	the soil water retention function [cm-1]	Parameter n in the soil water retention function [-]	Saturated Ks [cm/year]	Saturated Ks [cm/day]	Tortuosity parameter [-]
Layer 1	15,06	37,83	95,02	1,90	6,00	15,06	12,55	22,25	1,5	5	0,47	0,045	0,43	0,145	2,68	127750	350	0,5
Layer 2	9,75	24,49	61,53	1,23	3,88	9,75	8,13	14,41	1,5	5	0,47	0,045	0,43	0,145	2,68	127750	350	0,5
Layer 3	8,95	22,48	56,47	1,13	3,56	8,95	7,46	13,22	1,5	5	0,47	0,045	0,43	0,145	2,68	127750	350	0,5
Layer 4	7,65	19,22	48,29	0,96	3,05	7,65	6,38	11,31	1,5	5	0,47	0,119	0,35	0,014	2	255500	700	0,5
Layer 5	5,31	13,33	33,49	0,67	2,11	5,31	4,42	7,84	1,5	5	0,47	0,119	0,35	0,014	2	255500	700	0,5
Layer 6	10,58	26,59	66,79	1,33	4,21	10,58	8,82	15,64	1,5	5	0,47	0,119	0,35	0,014	2	255500	700	0,5
Layer 7	3,95	9,92	24,92	0,50	1,57	3,95	3,29	5,84	1,5	5	0,47	0,119	0,35	0,014	2	255500	700	0,5
Layer 8	3,15	7,91	19,86	0,40	1,25	3,15	2,62	4,65	1,5	5	0,47	0,119	0,35	0,014	2	255500	700	0,5
Layer 9	0,89	2,25	5,65	0,11	0,36	0,89	0,75	1,32	1,5	5	0,47	0,119	0,35	0,014	2	255500	700	0,5

Input parameters Hoornaar.

lay nr	Optie 1 PFOS + Lay	Optie 2 PFOS + Lay	Optie 1 PFOS + Lay	Optie 1 PFOA + Laagjes	Optie 2 PFOA + Laagjes	Optie 3 PFOA + Laagjes	PFOA best fit	PFOS best fit	Bulk density [g/cm3]	Dispersion [cm]	Molecular Diffusion [cm2/d]	Residual soil water content [-]	Saturated soil water content [-]	Parameter a in the soil water retention function [cm-	Parameter n in the soil water retention function [-]	Saturated Ks [cm/year]	Saturated Ks [cm/day]	Tortuosity parameter [-]
Layer 1	18,8	47,1	118,4	2,4	7,5	18,8	9,0	17,4	1,5	5	0,47	0,045	0,43	0,145	2,68	127750	350	0,5
Layer 2	17,1	42,9	107,7	2,1	6,8	17,1	8,2	15,8	1,5	5	0,47	0,045	0,43	0,145	2,68	127750	350	0,5
Layer 3	12,2	30,5	76,7	1,5	4,8	12,2	5,8	11,3	1,5	5	0,47	0,045	0,43	0,145	2,68	127750	350	0,5
Layer 4	4,4	11,0	27,6	0,6	1,7	4,4	2,1	4,1	1,5	5	0,47	0,119	0,35	0,014	2	255500	700	0,5
Layer 5	3,5	8,9	22,4	0,4	1,4	3,5	1,7	3,3	1,5	5	0,47	0,119	0,35	0,014	2	255500	700	0,5
Layer 6	1,4	3,6	9,0	0,2	0,6	1,4	0,7	1,3	1,5	5	0,47	0,119	0,35	0,014	2	255500	700	0,5
Layer 7	1,9	4,7	11,7	0,2	0,7	1,9	0,9	1,7	1,5	5	0,47	0,119	0,35	0,014	2	255500	700	0,5
Layer 8	1,2	3,1	7,8	0,2	0,5	1,2	0,6	1,1	1,5	5	0,47	0,119	0,35	0,014	2	255500	700	0,5
Layer 9	0,9	2,4	6,0	0,1	0,4	0,9	0,5	0,9	1,5	5	0,47	0,119	0,35	0,014	2	255500	700	0,5

Input parameters Schoonenburgsche heuvel.

lay nr	Optie 1 PFOS + Lay	Optie 2 PFOS + Lay	Optie 1 PFOS + Lay	Optie 1 PFOA + Laagjes	Optie 2 PFOA + Laagjes	Optie 3 PFOA + Laagjes	PFOA best fit	PFOS best fit	Bulk density [g/cm3]	Dispersion [cm]	Molecular Diffusion [cm2/d]	Residual soil water content [-]	Saturated soil water content [-]	Parameter a in the soil water retention function [cm-	Parameter n in the soil water retention function [-]	Saturated Ks [cm/year]	Saturated Ks [cm/day]	Tortuosity parameter [-]
Layer 1	73,6	184,8	464,2	9,3	29,3	73,6	86,1	203,3	0,63	5	0,47	0,034	0,46	0,016	1,37	7300	20	0,5
Layer 2	54,3	136,5	342,9	6,8	21,6	54,3	63,6	150,2	0,93	5	0,47	0,034	0,46	0,016	1,37	7300	20	0,5
Layer 3	224,9	564,9	1418,8	28,3	89,5	224,9	263,1	621,3	0,23	10	0,47	0,7	0,8	0,05	2	36500	100	0,5
Layer 4	233,0	585,2	1470,1	29,3	92,8	233,0	272,6	643,8	0,23	10	0,47	0,7	0,8	0,05	2	36500	100	0,5
Layer 5	190,7	479,0	1203,3	24,0	75,9	190,7	223,1	526,9	0,23	10	0,47	0,7	0,8	0,05	2	36500	100	0,5
Layer 6	189,8	476,7	1197,5	23,9	75,6	189,8	222,0	524,4	0,23	10	0,47	0,7	0,8	0,05	2	36500	100	0,5
Layer 7	198,8	499,3	1254,1	25,0	79,1	198,8	232,6	549,2	0,23	10	0,47	0,7	0,8	0,05	2	36500	100	0,5

Input parameters Schoonenburgsche heuvel peat.

Ondertekening

Utrecht. 12-02-2021 TNO

D. Maljers.
Afdelingshoofd

T.G.J.Gerardu
Auteur